

Structural Bases for Substrate and Inhibitor Recognition by Matrix Metalloproteinases

Loretta Aureli^{*1}, Magda Gioia², Ilaria Cerbara¹, Susanna Monaco^{2,3}, Giovanni Francesco Fasciglione², Stefano Marini², Paolo Ascenzi^{4,5}, Alessandra Topai^{*1} and Massimo Coletta^{*2,3}

¹Colosseum Combinatorial Chemistry Centre for Technology (C4T S.C.a r.l.), Via della Ricerca Scientifica s.n.c., I-00133 Roma, Italy; ²Department of Experimental Medicine and Biochemical Sciences, University of Roma Tor Vergata, Via Montpellier 1, I-00133 Roma, Italy; ³Interuniversity Consortium for the Research on the Chemistry of Metals in Biological Systems (CIRCMSB), Via C. Ulpani 27, I-70125 Bari, Italy; ⁴Interdepartmental Laboratory for Electron Microscopy, University Roma Tre, Via della Vasca Navale 79, I-00146 Roma, Italy and ⁵National Institute for Infectious Diseases I.R.C.C.S. 'Lazzaro Spallanzani', Via Portuense 292, I-00149 Roma, Italy

Abstract: Matrix metalloproteinases (MMPs) are a family of zinc-dependent endopeptidases which are involved in the proteolytic processing of several components of the extracellular matrix. As a consequence, MMPs are implicated in several physiological and pathological processes, like skeletal growth and remodelling, wound healing, cancer, arthritis, and multiple sclerosis, raising a very widespread interest toward this class of enzymes as potential therapeutic targets. Here, structure-function relationships are discussed to highlight the role of different MMP domains on substrate/inhibitor recognition and processing and to attempt the formulation of advanced guidelines, based on natural substrates, for the design of inhibitors more efficient *in vivo*.

Keywords: Matrix metalloproteinases, Enzyme-substrate recognition, Enzyme-inhibitor recognition, Structural bases.

1. INTRODUCTION

Matrix metalloproteinases (MMPs) are a family of approximately 27 Zn²⁺ ion-dependent endopeptidases which are involved in the proteolytic processing of several components of the extracellular matrix, such as collagens, proteoglycans and fibronectin [1-3].

Since MMPs are able to degrade basement membranes and extracellular matrix components, they have traditionally been viewed as effectors of late stage of cancer evolution. However, MMPs also have an important regulatory role, as they can modulate cytokine and chemokine activity by proteolytic processing [4-7]. Therefore, MMPs are implicated in several physiological and pathological processes, like skeletal growth and remodelling, wound healing, cancer, arthritis and multiple sclerosis [8-13], raising a very widespread interest toward this class of enzymes as potential therapeutic targets [14].

MMPs are virtually able to enzymatically process all molecules present in the extracellular matrix, although displaying very different propensity for various substrates [1,3]. However, since the most common substrate present in the extracellular matrix is collagen, in the following classification we use it as a comparison substrate element among different classes of MMPs. On this basis, MMPs are usually classified into five main groups, namely:

- 1) Collagenases (i.e., MMP-1, MMP-8 and MMP-13), which are able to preferentially cleave fibrillar

collagen, recognizing the substrate through the haemopexin-like domain [15-17].

- 2) Gelatinases (i.e., MMP-2 and MMP-9), which are able to enzymatically process various substrates of the extracellular matrix (ECM), such as collagen I and collagen IV. Beside the haemopexin-like domain, these MMPs are characterized by the presence of an additional domain, called collagen binding domain (CBD) and located in their catalytic domain. CBD is made of three fibronectin II-like repeats and represents the preferential binding domain for fibrillar collagen I [18].
- 3) Stromelysins (i.e., MMP-3, MMP-10 and MMP-11), which are able to hydrolyse collagen IV, but do not cleave fibrillar collagen I [1].
- 4) Matrilysins (i.e., MMP-7 and MMP-26), which lack the haemopexin-like domain and are able to process collagen IV but not collagen I [19, 20].
- 5) Membrane-type (MT-MMPs) (i.e., MMP-14, MMP-15, MMP-16, MMP-17 and MMP-24), which contain at the C-terminal an additional domain, represented by an intermembrane region, completed by a short cytoplasmic tail. Only MMP-14 has been shown to be able to cleave fibrillar collagen I [21].

Finally, there are few MMPs, such as metalloelastase (MMP-12) and epilysin (MMP-28), which cannot be included in any of the above mentioned classes, and which will be treated separately.

In view of the MMP involvement in several pathological processes, the development of powerful and selective inhibitors might represent an important therapeutic goal, this being especially relevant for cancer therapy [22-24]. However, recent failures of MMP inhibitors in cancer clinical trials [25] have raised a question on MMPs druggability, mostly

*Address correspondence to these authors at the ¹Colosseum Combinatorial Chemistry Centre for Technology (C4T S.C.a r.l.), Via della Ricerca Scientifica s.n.c, I-00133 Roma, Italy; Tel: +39/0672594029;

Fax: +39/0672594031;

E-mail: alessandra.topai@uniroma2.it; loretta.aureli@uniroma2.it

²Department of Experimental Medicine and Biochemical Sciences, University of Roma Tor Vergata, Via Montpellier 1, I-00133 Roma, Italy; Tel: +39/0672596365; Fax: +39/0672596353;

E-mail: coletta@seneca.uniroma2.it

because of their multiple and often contradictory role in cancer disease [14,26].

In spite of these problematic aspects, the relevance of the physiopathological role of MMPs is unquestionable, keeping unaltered their importance as potential druggable targets, even though a better knowledge is needed to understand which (and when) a MMP is actually involved in a specific pathological process [26]. On the other hand, previous failures of MMP inhibitors as drugs can also be likely overcome by addressing the design of inhibitors toward both (i) a higher selectivity for different MMPs (in order to inhibit only the target MMP) and (ii) interaction with multiple recognition sites on a given MMP. The last point concerns the fact that up to now inhibitors have been only designed to fit into the active site of MMPs, following the concept that the crucial requirement is to impair the bond cleavage. However, a growing information is building up on the relevant catalytic role played also by non-catalytic MMP domains, which regulate the recognition of macromolecular substrates. Therefore, they appear as invaluable candidates for specific MMP inhibition *in vivo*. [15,16,27-31].

In the framework of these considerations, this study overviews comparatively three-dimensional structures (3D) of MMPs, aiming to provide structural similarities and differences among all family members, in order to unravel structural features of the MMP substrate binding sites needed for the selective inhibitors design. Beside a selection of synthetic inhibitors, the structural bases of the MMPs interaction with natural inhibitors (such as Tissue Inhibitors of Metallo-Proteinase (TIMPs)) have been examined, in order to identify the main determinants of macromolecular recognition. Furthermore, a limited set of examples has been illustrated to outline differences in natural substrates and synthetic inhibitor recognition, as well as in enzymatic processing. As a whole, the guidelines for further steps in MMP inhibitor design are formulated.

2. STRUCTURAL ASPECTS OF MMPS AND OF MMP-SYNTHETIC INHIBITOR COMPLEXES

2.1. The Overall MMP Structural Organization

Currently, updated to December 2007, the RCSB Protein Structure Databank counts about 130 MMPs 3D structures, either ligand free and/or complexed with a specific synthetic or natural inhibitor [see <http://www.rcsb.org/pdb/>] [32]. A comprehensive list of all structures available to date for the MMP family and for TIMPs is reported in Tables 1A and 1B. All MMP structures show the characteristic fold of zinc-dependent endopeptidases (Fig. 1), consisting of three α -helices, four parallel β -sheet strands and one anti-parallel β -sheet strand [33].

Sequence comparison of MMPs reveals consistent similarities in their domain organization (Fig. 2), which is usually made by: (i) the pre-peptide involved in the pro-enzyme secretion process, (ii) the auto-inhibitory pro-domain, (iii) the catalytic domain and (iv) the C-terminal haemopexin-like domain often involved in the recognition/positioning of substrates (Figs. 1 and 2).

All MMPs structures contain in the active site the common sequence motif His-Glu-Xxx-Gly-His-Xxx-Xxx-Gly-Xxx-Xxx-His, where three His residues coordinate the catalytic Zn^{2+} ion [34].

The catalytic domain is connected to the haemopexin-like domain by a segment, called linker or hinge region [35]. This connecting linker might fulfil important functional roles rather than simply acting as physical spacer, since it turns out to be important for the stability of the enzyme and for the degradation of substrates [36], this being especially true for the collagenase family [37].

The pro-domain, composed of about 80 residues, extends from the N-terminus to the catalytic domain and it is responsible for the enzyme latency. A cysteine sulphhydryl group present in the N-terminal pro-domain (i.e., "Cys-switch": Pro-Arg-Cys-Gly-Xxx-Pro-Asp) interacts with the Zn^{2+} ion and blocks the active site [38]. The pro-domain of some MMPs shows a recognition sequence for furin-like serine proteinases, which is needed for the pro-domain cleavage and, consequently, for the MMPs activation [39].

The haemopexin-like C-terminal domain is composed of four β -sheets, each forming a blade of the four-bladed β -propeller structure [34]. On the other hand, MMP-7 and MMP-26 are lacking the haemopexin domain, while the recently reported MMP-23 has an immunoglobulin-like domain replacing the haemopexin repeat [40].

Further, MMP-2 and MMP-9 show an additional domain (called fibronectin-like domain), inserted within the catalytic region and involved in the collagen recognition [39].

Moreover, some MT-MMPs contain either a membrane anchor (such as MMP-17 and MMP-25, which are anchored to the membrane through a C-terminal glycosylphosphatidylinositol moiety, and MMP-23, which is anchored to the membrane at the N-terminus) or a cytoplasmic domain at the C-terminus (such as MMP-14, MMP-15, MMP-16 and MMP-24) [41].

The overall topology of the MMP catalytic domain is spherical, with (i) the catalytic Zn^{2+} ion coordinated by three His residues, (ii) a structural Zn^{2+} coordinated by three His and one Asp residues, and (iii) at least two structural calcium atoms octahedrally coordinated, which stabilise the whole architecture [33].

In unliganded MMPs, the catalytic zinc residing in its center is coordinated by three imidazole $N_{\epsilon 2}$ atoms of the three His and by a fixed water molecule, which is simultaneously at a hydrogen bond distance to the carboxylate group of the catalytic Glu residue, conserved in all MMPs. Conversely, in the case of MMP complexes with bidentate inhibitors (i.e., those with an hydroxamic acid function) this water is replaced by two oxygen atoms, which together with the three imidazoles bind the catalytic Zn^{2+} ion in a trigonal-bipyramidal (pentacoordinate) manner. Additionally, a conserved Met residue, forming a "Met-turn", contributes to protect the catalytic zinc [34].

The growing availability of MMP 3D structures has contributed to develop and speed up the drug design process, which can now exploit realistic molecular modelling procedures [42]. In the past, drug design research focussed on tar-

Table 1. Data Set of the MMP Experimental Structures Available at Protein Data Bank**(A) Humans**

Subfamily	(Pro) enzyme	Structure type	PDB code	Resolution (Å)	Domains	Ligands ^a	References
Collagenase	MMP-1	X-ray	2clt	2.70	Full length	Ligand-free	[47]
		X-ray	1su3	2.20	Pro MMP-1 Full length	Ligand-free	[48]
		X-ray	1cge	1.90	Catalytic	Ligand-free	[49]
		X-ray	1cgf	2.10	Catalytic	Ligand-free	[49]
		X-ray	1cgl	2.04	Catalytic	EMR	[50, 51]
		X-ray	966c	1.09	Catalytic	RS2	[52]
		X-ray	2tcl	2.02	Catalytic	RO4	[53]
		X-ray	1hfc	1.56	Catalytic	HAP	[54]
		NMR	1ayk - 2ayk ^b	---	Catalytic	Ligand-free	[55, 56]
		NMR	3ayk ^b - 4ayk	---	Catalytic	CGS	[57]
	MMP-8	X-ray	1zvx	1.60	Catalytic	FIN	[62]
		X-ray	1zs0	1.90	Catalytic	EIN	[62]
		X-ray	1bzs	1.70	Catalytic	BSI	[63]
		X-ray	1ji9	2.00	Catalytic	BBT	[64]
		X-ray	1mmb	2.10	Catalytic	BAT	[65]
		X-ray	1jap	1.80	Catalytic	HOA	[66]
		X-ray	1a85 - 1a86	2.00	Catalytic	HMI	[67]
		X-ray	1zp5	1.80	Catalytic	2NI	[68]
		X-ray	1i73	1.40	Catalytic	PAT	[69]
		X-ray	1i76	1.20	Catalytic	BSI	[69]
MMP-13	X-ray	1kbc	1.80	Catalytic	HLE	[70]	
	X-ray	1jh1	2.70	Catalytic	JST	[71]	
	X-ray	2oy4	1.70	Catalytic	Ligand-free	[72]	
	X-ray	1jan	2.50	Catalytic	HOA	[73]	
	X-ray	1jaq	2.40	Catalytic	HMP	[74]	
	X-ray	1jao	2.40	Catalytic	GM1	[74]	
	X-ray	1mnc	2.10	Catalytic	PLH	[75]	
	X-ray	830c	1.60	Catalytic	RS1	[52]	
	X-ray	1xuc	1.70	Catalytic	PB3	[76]	
	X-ray	1xud	1.80	Catalytic	PB4	[76]	
	X-ray	1xur	1.80	Catalytic	PB5	[76]	
	X-ray	2ow9	1.70	Catalytic	SP6	[77]	
	X-ray	2ozr	2.30	Catalytic	HAE	[77]	
	X-ray	2d1n	2.40	Catalytic C-terminal	FA4	[78]	
	NMR	1eub	---	Catalytic	MSB	[79]	
	X-ray	456c	2.40	Catalytic	345	[52]	
	NMR	1fm1-1fls	---	Catalytic	WAY	[80]	

(Table 1A). contd.....

Subfamily	(Pro) enzyme	Structure type	PDB code	Resolution (Å)	Domains	Ligands ^a	References
		X-ray	1ztq	2.00	Catalytic	O33	[81]
		X-ray	1pex	2.70	Haemopexin-like	Ligand-free	[82]
		X-ray	1you	2.30	Catalytic	PFD	[83]
Gelatinase	MMP-2	X-ray	1ck7	2.08	Pro MMP-2	Ligand-free	[92]
		X-ray	1gen	2.01	Haemopexin-like	Ligand-free	[96]
		X-ray	1rtg	2.06	Haemopexin-like	Ligand-free	[97]
		NMR	1hov	---	Catalytic	I52	[98]
		X-ray	1qib	2.08	Catalytic	Ligand-free	[99]
		NMR	1ks0	---	Fibronectin Type II	Ligand-free	[100]
		X-ray	1eak	2.07	Pro MMP-2 Catalytic	Ligand-free	[92]
	MMP-9	X-ray	1l6j	2.50	Pro MMP9 C-Truncated	Ligand-free	[102]
		X-ray	1itv	1.95	Haemopexin-like	Ligand-free	[103]
		X-ray	2ovx-2ovz- 2ow0	2.00	Catalytic	4MR-5MR- 6MR	[104]
		X-ray	2ow1	2.02	Catalytic	7MR	[104]
		X-ray	2ow2	2.09	Catalytic	8MR	[104]
		X-ray	1gkc	2.03	Catalytic	BUM	[93]
		X-ray	1gkd	2.01	Catalytic	STN	[93]
Stromelysin	MMP-3	X-ray	1slm	1.90	Pro-MMP3	Ligand-free	[105]
		X-ray	1sln	2.27	Catalytic	INH	[105]
		X-ray	1hy7	1.50	Catalytic	MBS	[106]
		X-ray	1usn	1.80	Catalytic	IN9	[107]
		X-ray	2usn	2.20	Catalytic	IN8	[107]
		NMR	3usn	----	Catalytic	ATT	[108]
		X-ray	1c3i	1.83	Catalytic	TR1	[109]
		X-ray	1ciz	1.64	Catalytic	DPS	[110]
		X-ray	1caq	1.80	Catalytic	DPS	[110]
		X-ray	1b8y	2.00	Catalytic	IN7	[110]
		X-ray	1qia - 1qic	2.00	Catalytic	Ligand-free	[110]
		X-ray	1d7x	2.00	Catalytic	SPC	[111]
		X-ray	1g49	1.90	Catalytic	111	[112]
		X-ray	1hfs	1.70	Catalytic	L04	[113]
		X-ray	1d8f	2.40	Catalytic	SPI	[114]
		X-ray	1d5j	2.60	Catalytic	MM3	[115]
		X-ray	1d8m-1g05	2.45	Catalytic	BBH	[116]
		X-ray	2d1o	2.02	Catalytic C-terminal	FA4	[78]
		X-ray	1b3d	2.30	Catalytic	S27	[117]

(Table 1A). contd.....

Subfamily	(Pro) enzyme	Structure type	PDB code	Resolution (Å)	Domains	Ligands ^a	References
		X-ray	1cqr	2.00	Catalytic	Ligand-free	[117]
		NMR	1bm6	----	Catalytic	MSB	[118]
		NMR	1ums - 1umt	----	Catalytic	HAE	[119]
		X-ray	1bqo	2.30	Catalytic Truncated	N25	[120]
		X-ray	1biw	2.50	Catalytic	S80	[121]
		NMR	2srt	----	Catalytic	INH	[122]
		X-ray	1g4k	2.00	Catalytic	HQQ	[123]
		NMR	2jnp	----	Catalytic	NGH	[124]
		NMR	2jt5	----	Catalytic	MLC	[124]
		NMR	2jt6	----	Catalytic	InhVII	[124]
	MMP-10	X-ray	1q3a	2.10	Catalytic	NGH	[125]
Matrilysin	MMP-7	X-ray	1mmq	1.90	Catalytic	RRS	[129]
		X-ray	1mmp	2.30	Catalytic	RSS	[129]
		X-ray	1mmr	2.40	Catalytic	SRS	[129]
		NMR	2ddy	----	Catalytic	MDW	http://www.rcsb.org/pdb/
MT-MMP	MMP-16	X-ray	1rm8	1.80	Catalytic	BAT	[136]
Metallo elastase	MMP-12	X-ray	1jiz	2.60	Catalytic	CGS	[140]
		X-ray	1y93	1.03	Catalytic	HAE	[141]
		X-ray	1rmz	1.34	Catalytic	NGH	[141]
		NMR	1ycm-1z3j	---	Catalytic	NGH	[141]
		X-ray	1utz	2.50	Catalytic	PF3	[142]
		X-ray	1utt	2.20	Catalytic	CP8	[142]
		X-ray	1ros	2.00	Catalytic	DEO	[142]
		X-ray	1jk3	1.09	Catalytic	BAT	[143]
		X-ray	2oxu	1.24	Catalytic	Ligand-free	[144]
		X-ray	2oxz	1.90	Catalytic	Ligand-free	[144]
		X-ray	2oxw	1.15	Catalytic	Ligand-free	[144]
		X-ray	2hu6	1.32	Catalytic	HAE	[145]
		X-ray	1os2	2.15	Catalytic	HAE	[146]
		X-ray	1os9	1.85	Catalytic	Ligand-free	[146]
		NMR	2poj	----		Ligand-free	[147]
TIMP	TIMP-1	NMR	1d2b	----	N-terminal	----	[158]
	MMP3/ TIMP-1	X-ray	1uea	2.80	Catalytic/ N-terminal	----	[159]
	MMP3/ TIMP-1	NMR	1oo9	----	Catalytic/ N-terminal	----	[160]
	MMP1/ TIMP-1	X-ray	2jot	2.54	Catalytic/ N-terminal	----	[161]
	TIMP-2	X-ray	1br9	2.10	Full length	----	[162]
	TIMP-2	NMR	2tmp	----	N-terminal	----	[163]
	ProMMP2/TI MP-2	X-ray	1gxd	3.10	Haemopexin- like	----	[165]

All proteins are from human source.

^aLigands have been identified according to 'PDB-Ligand' available at: <http://www.idrtech.com/PDB-Ligand>.

^bNMR minimised structures.

(B) Other Mammals

Subfamily	(Pro) enzyme	Structure type	PDB Code	Resolution (Å)	Comments	Ligands ^a	References
Collagenase	MMP-1	X-ray	1fbl	2.50	Full length ^b	HTA	[58]
	MMP-13	X-ray	1cxv	2.00	Catalytic ^c	CBP	[84]
Stromelysin	MMP-11	X-ray	1hv5	2.60	Catalytic ^c	CPS	[126]
TIMP	MMP-14/ TIMP-2	X-ray	1bqq-1buv	2.75	Catalytic/ Full length TIMP-2 ^d	----	[139]
	MMP-13/ TIMP-2	X-ray	2ed2	2.00	Catalytic/ N-terminal TIMP-2 ^d	----	[166]

^aLigands have been identified according to 'PDB-Ligand' available at: <http://www.idrtech.com/PDB-Ligand>.

^bporcine.

^cmurine.

^dbovine.

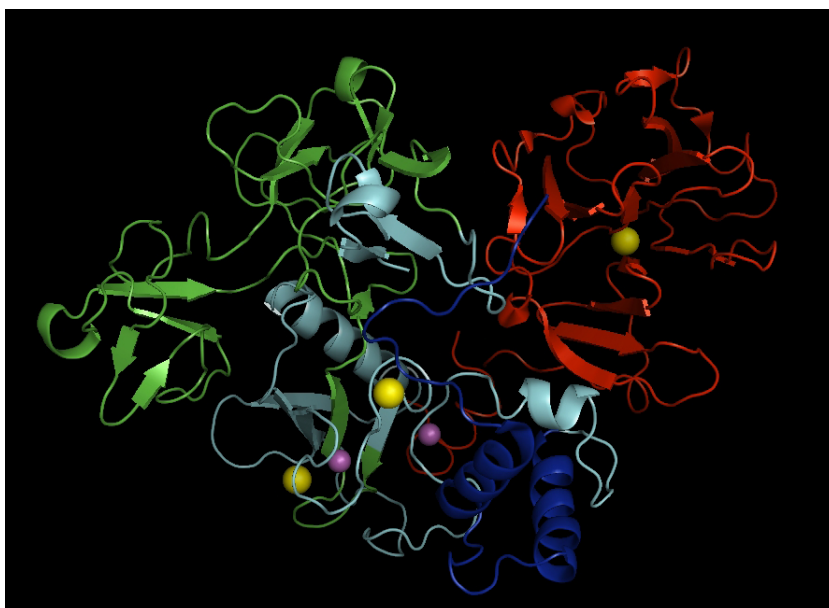


Fig. (1). Ribbon structure of the human full length MMP-2 (PDB code:1ck7). The pro-domain is displayed in blu, the catalytic domain in cyan, the haemopexin-like C-terminal domain in red, the fibronectin-like domain in green. The zinc and calcium ions are displayed as yellow and pink spheres, respectively. The snapshot was made by PyMol software [205].

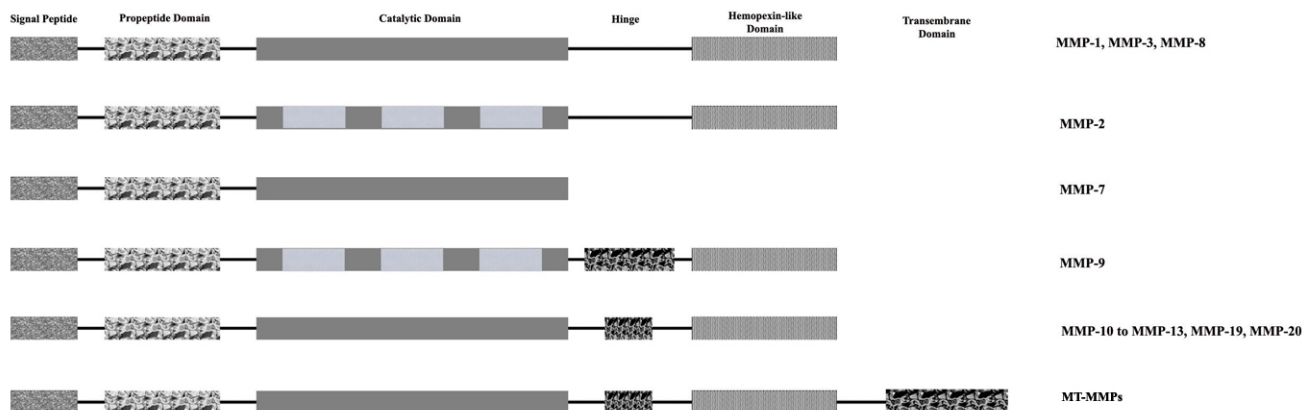


Fig. (2). Schematic representation of the domain topology of MMP family members.

getting the MMP catalytic domain complexed with peptidic, peptidomimetic, and non-peptidic inhibitors [39, 42-45]. However, since the MMP 3D structure is remarkably well conserved, the design of highly specific inhibitors which selectively interact with a specific MMP is to date very difficult, even though relevant differences for the intrinsic flexibility of the catalytic domain can explain the selective recognition within a given subclass of MMPs [42].

The active site cleft consists of several recognition pockets, half of which are located on the right side of the catalytic Zn^{2+} ion (called primed side, with pockets named S'_n and $n = 1, 2, \dots, n$) and the rest on the left side of the catalytic Zn^{2+} ion (called unprimed side, with pockets named S_n and $n = 1, 2, \dots, n$). By analogy P_1' , referring to substrate and/or inhibitor, shows a generic chemical group able to fit into the S_1' pocket [43].

Usually, the most important recognition site (at least for small synthetic substrates and inhibitors) is the primary hydrophobic S_1' pocket, which is characterized by a variable length amino acid composition and conformation (according to the different MMPs), followed by shallow S_2' and S_3' pockets, which are primarily exposed to the solvent. For all MMPs, the size and shape of the S_1' specific pocket critically regulates the ligand binding selectivity, such that MMPs generally fall in two classes [33, 39, 44]:

- 1) Those with a large and open S_1' pocket, such as MMP-2, MMP-3, MMP-8, MMP-9, MMP-12 and MMP-13;
- 2) Those with a small S_1' pocket, such as MMP-1 and MMP-7.

In MMPs belonging to the first group, the S_1' pocket is preformed, wide and more able to accommodate large P_1' groups. Conversely, in MMPs belonging to the second class the S_1' pocket is smaller and not preformed, since it is occluded by either Arg²¹⁴ or Tyr²¹⁴, respectively [39]. Note that, although large P_1' groups are not excluded to be recognized by the so-called small S_1' pocket, their binding requires an induced-fit open conformation, as observed in MMP-1 (see below).

A comparison of the 3D structural similarities and differences for the most representative MMP family members and MMP/TIMP complexes is described below.

In particular, for each subfamily member we have selected at least one 3D complex deposited at the Protein Data Bank according to the following criteria:

- 1) the complexes with the highest resolution;
- 2) preference was given to proteins from human source;
- 3) proteins complexed with a known inhibitor and/or ligand-free.

2.2. Collagenases

The collagenase family includes three important members: MMP-1, MMP-8 and MMP-13. A list of their experimental structures, either ligand-free and/or co-crystallised with some inhibitor is reported in Table (1A and B).

The main difference between MMP-1, MMP-8 and MMP-13 concerns the shape and size of the well defined S_1'

pocket. The S_1' binding pocket of MMP-1 is significantly occluded by the Arg²¹⁴ residue, while that of MMP-8 is larger and more open, being formed by Leu¹⁶⁰ and Ala¹⁶¹ residues [46]. On the other hand, the MMP-13 S_1' pocket is a long and open channel able to easily accommodate large P_1' groups [see paragraph 2.2.3]. The contour of this tunnel is dominated by Leu²¹⁸ and by the conformation of residues 244-255, which render the S_1' site larger than in other MMPs, forming the so called " $S_1'^*$ specificity loop" [see paragraph 2.2.3].

2.2.1. MMP-1 (Collagenase-1)

The RCSB PDB for MMP-1 counts, to date, thirteen 3D structures [47-58], (see Tables 1A and B).

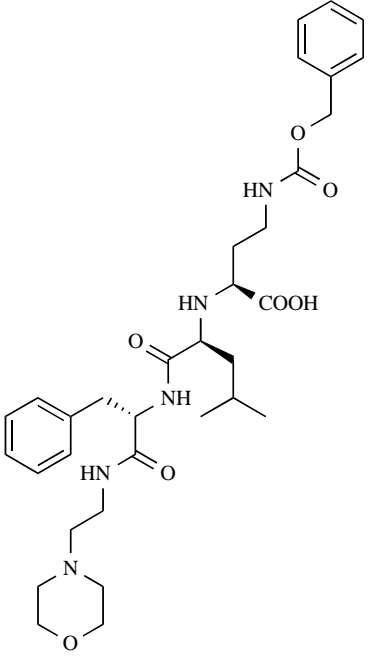
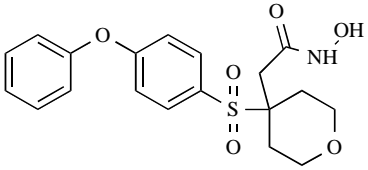
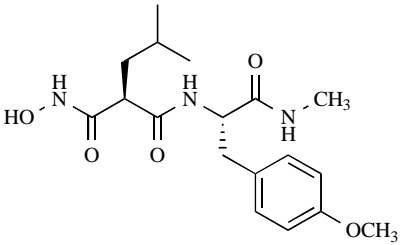
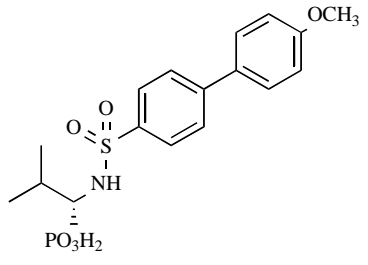
The X-ray structure of the active form of ligand-free human full length MMP-1 is reported at a 2.7 Å resolution (2clt.pdb) [47]. The close similarity between this 3D structure and that of the isolated catalytic domain indicates that the removal of the haemopexin-like domain does not perturb significantly the structure [47]. On the other hand, significant structural differences can be detected by comparing the full-length active MMP-1 with the human proMMP-1, determined at 2.2 Å resolution (1su3.pdb) [48], mainly referable to the topological interaction between the pro-peptide (not present in the active enzyme) and the haemopexin-like domain. Since the proteolytic activity of MMP-1 requires that the haemopexin-like domain binds the substrate [15, 30], the reduced activity of proMMP-1 derives from its closed conformation which impairs the binding of the collagen peptide by the haemopexin-like domain [48].

Looking more closely at the active site of MMP-1 and in particular focussing on the S_1' pocket, it is interesting to outline that in MMP-1 Asn¹⁶³ makes the site less hydrophobic than in other MMPs, which display a Leu, or Val, or Ile residue at the same position [59].

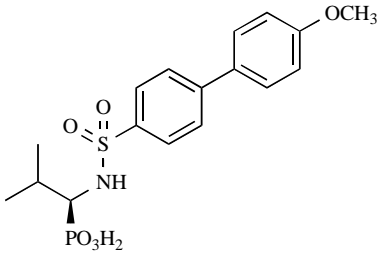
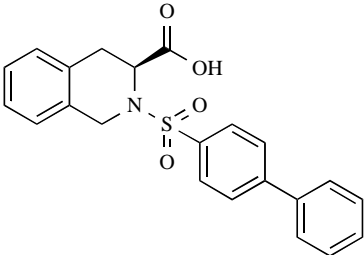
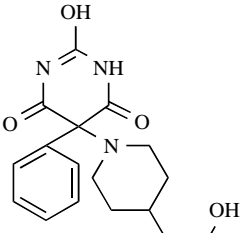
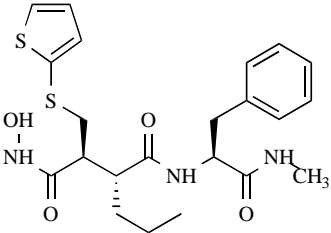
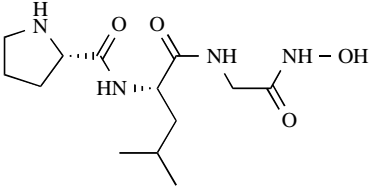
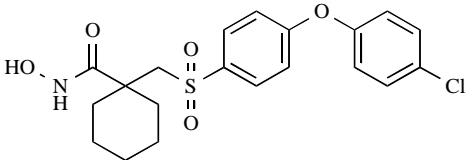
The earliest MMP inhibitors were designed on the basis of the amino acid sequence encompassing the site of cleavage of human triple helical collagen by MMP-1. On this substrate-based design approach, three classes of compounds have been developed: (i) inhibitors interacting with both the right and left sides, (ii) inhibitors binding to the left-hand side only and (iii) inhibitors binding to the right-hand side of the catalytic center [43]. A wide variety of MMP inhibitors, classified according to this approach and incorporating a range of different Zinc Binding Groups (ZBG), has been reported previously [43,60,61]. It was generally found that compounds which mimic the sequence of the right-hand primed side of the active site (i.e., $P_1' - P_2' - P_3'$) and incorporate a hydroxamic acid ZBG showed strong inhibitory properties. In contrast, a modest inhibitory potency was reported for the left-hand unprimed side inhibitors (i.e., $P_1 - P_2 - P_3$) [43,60,61].

The X-ray crystal structure at 2.04 Å resolution of the hMMP-1 catalytic domain bound to a peptidic carboxylic acid inhibitor (1 in Table 2) is described (1cgl.pdb) [50,51]. The structure encloses (Fig. (3a)): a central carboxylate group, which binds the catalytic Zn^{2+} ion, P_1' (leucine), P_2' (phenylalanine), P_3' (morpholine), and P_1 (benzyloxycarbonylamino group, which is hydrogen bonded to Asn¹⁸⁰ on the unprimed side of the active site cleft).

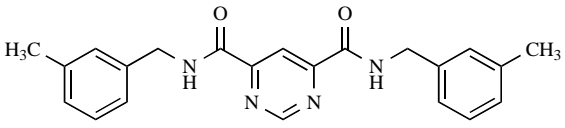
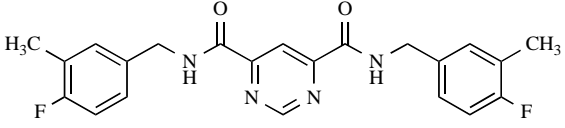
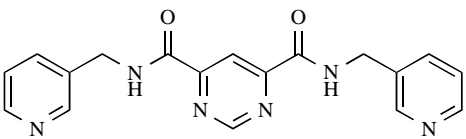
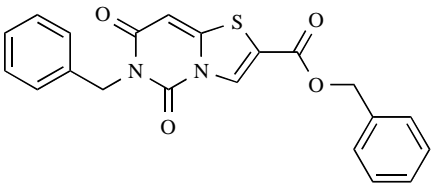
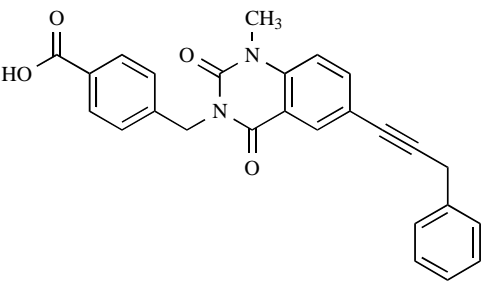
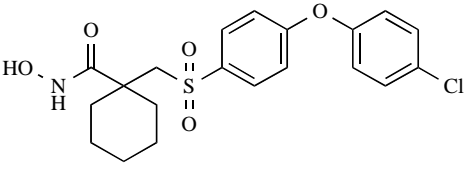
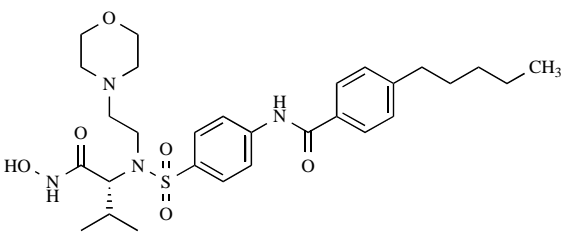
Table 2. Chemical 2D Structures of Some MMP Inhibitors

Structure	Inhibitor type	PDB code	K _i (nM) or IC ₅₀ (nM)	Ref.
 <p>1</p>	Peptidic carboxylic acid	1cgl	K _i = 135 (MMP-1)	[50, 51]
 <p>2</p>	sulfone hydroxamic acid	966c	K _i = 23 (MMP-1)	[52]
 <p>3</p>	hydroxamic acid	1flb	No functional data are available	[58]
 <p>4</p>	(R)-sulfonamide phosphonate	1zvx	K _i = 0.6 (MMP-8)	[62]

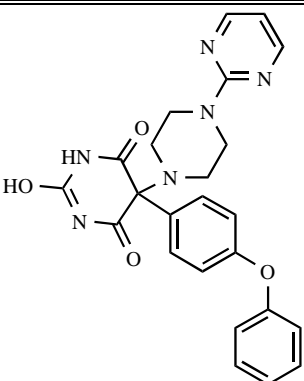
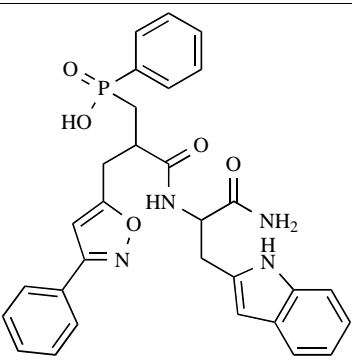
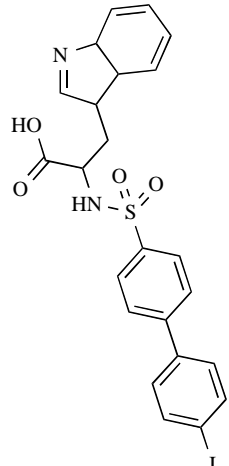
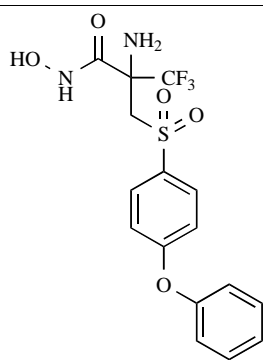
(Table 2). Contd.....

Structure	Inhibitor type	PDB code	K _i (nM) or IC ₅₀ (nM)	Ref.
 <p>5</p>	(S)-sulfonamide phosphonate	1zs0	K _i = 700 (MMP-8)	[62]
 <p>6</p>	carboxylic acid	1bzs	IC ₅₀ = 10 (MMP-8)	[63]
 <p>7</p>	barbiturate ring	1ij9	IC ₅₀ = 700 (MMP-8)	[64]
 <p>8</p>	hydroxamic acid	1mmb-1rm8-1jk3	IC ₅₀ = 5 (MMP-8)	[65, 136, 143]
 <p>9</p>	Pro-Leu- Gly hydroxylamine	1jap	IC ₅₀ = 700 (MMP-8)	[66]
 <p>10</p>	sulphone hydroxamic acid	830c	K _i = 0.52 (MMP-13)	[52]

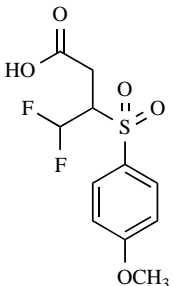
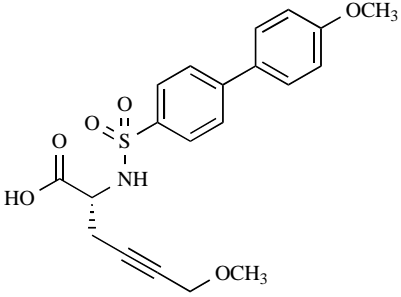
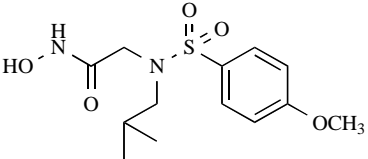
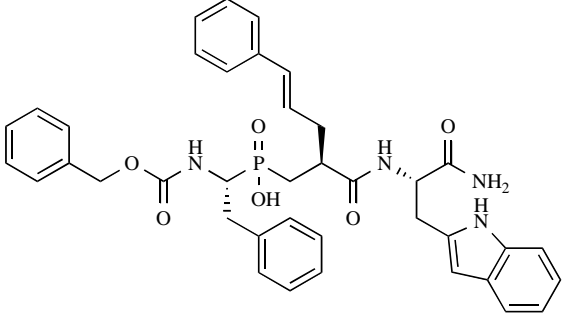
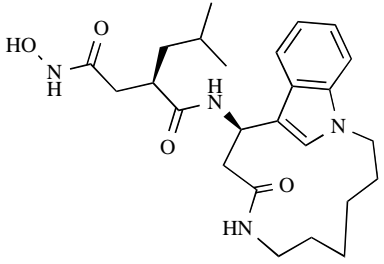
(Table 2). Contd.....

Structure	Inhibitor type	PDB code	K _i (nM) or IC ₅₀ (nM)	Ref.
 <p style="text-align: center;">11</p>	pyrimidine dicarboxamide	1xuc	IC ₅₀ = 72 (MMP-13)	[76]
 <p style="text-align: center;">12</p>	pyrimidine dicarboxamide	1xud	IC ₅₀ = 8 (MMP-13)	[76]
 <p style="text-align: center;">13</p>	pyrimidine dicarboxamide	1xur	IC ₅₀ = 400 (MMP-13)	[76]
 <p style="text-align: center;">14</p>	pyrimidin benzyl ester	2ow9	IC ₅₀ = 30 (MMP-13)	[77]
 <p style="text-align: center;">15</p>	carboxylic acid	2ozr	IC ₅₀ = 0.67 (MMP-13)	[77]
 <p style="text-align: center;">16</p>	sulfone hydroxamic acid	1cxv	No functional data are available	[84]
 <p style="text-align: center;">17</p>	sulfonamide hydroxamic acid	1hov	No functional data are available	[98]

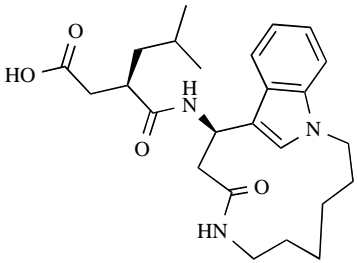
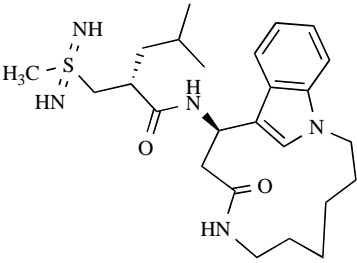
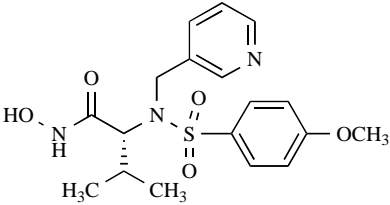
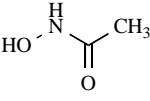
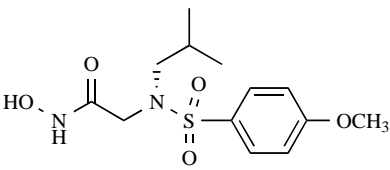
(Table 2). Contd.....

Structure	Inhibitor type	PDB code	K _i (nM) or IC ₅₀ (nM)	Ref.
 <p style="text-align: center;">18</p>	barbiturate ring	2ovx	IC ₅₀ = 2 (MMP-9)	[104]
 <p style="text-align: center;">19</p>	phosphinic acid	2ovz	K _i = 13 (MMP-9)	[104]
 <p style="text-align: center;">20</p>	carboxylic acid	2ow0	IC ₅₀ = 201 (MMP-9)	[104]
 <p style="text-align: center;">21</p>	hydroxamic acid	2ow1	IC ₅₀ = 1.0 (MMP-9)	[104]

(Table 2). Contd.....

Structure	Inhibitor type	PDB code	K _i (nM) or IC ₅₀ (nM)	Ref.
 <p>22</p>	carboxylic acid	2ow2	IC ₅₀ = 6 (MMP-9)	[104]
 <p>23</p>	sulfonamide carboxylic acid	1hy7	No functional data are available	[106]
 <p>24</p>	sulfonamide hydroxamic acid	1q3a	K _i = 0.6 (MMP-10)	[125]
 <p>25</p>	phosphinic	1hv5	K _i = 700 (MMP-11)	[126]
 <p>26</p>	hydroxamic acid	1mmq	K _i = 30 (MMP-7)	[129]

(Table 2). Contd.....

Structure	Inhibitor type	PDB code	K_i (nM) or IC_{50} (nM)	Ref.
 <p>27</p>	carboxylic acid	1mmp	$K_i = 850$ (MMP-7)	[129]
 <p>28</p>	sulfodiimine	1mmr	$K_i = 4000$ (MMP-7)	[129]
 <p>29</p>	sulfonamide hydroxamic acid	1jiz	$IC_{50} = 700$ (MMP-12)	[140]
 <p>30</p>	hydroxamic acid	1y93	$K_i = 0.52$ (MMP-12)	[141]
 <p>31</p>	sulfonamide hydroxamic acid	1rmz-1ycm-1z3j	$IC_{50} = 72$ (MMP-12)	[141]

The X-ray structure of the hMMP-1 catalytic domain, complexed with a sulfone hydroxamic acid (**2** in Table 2) at 1.09 Å resolution (Fig. (3b)), provides the basis for understanding the selectivity profile of inhibition (966c.pdb) [52]. This selectivity is primarily due to the size and shape of the S'_1 pocket, which is relatively small and whose depth is limited at the bottom by the residue Arg²¹⁴, which occupies a position equivalent to that of the residue Leu²¹⁸ in MMP-13.

Given the small S'_1 pocket, it is somewhat surprising to find some large P_1' groups as potent MMP-1 inhibitors. In particular, it is interesting to outline that in this inhibitor (**2** in Table 2) the presence of a diphenylether P_1' substituent induces a conformational change of Arg²¹⁴, whose new position creates a larger and open channel, clearly envisaging the

possibility for the inhibitor to alter the substrate recognition site [52].

The crystal structure of full-length porcine MMP-1, complexed with a hydroxamic acid inhibitor (**3** in Table 2), is also available at 2.5 Å resolution (1fbl.pdb) [58]. The visual inspection of this structure allows to identify two domains connected through an exposed proline-rich and flexible linker of 17 amino acids. Porcine MMP-1 shows a 87.6 % identity with the human enzyme and a close similarity of the catalytic domain backbone with respect to the human MMP-1 and MMP-8 [58]. However, when full-length human and porcine MMP-1 have been superimposed on the basis of the catalytic domain, a variation by 1.2 Å for the haemopexin-like C-terminal domain shows up. Thus, in porcine

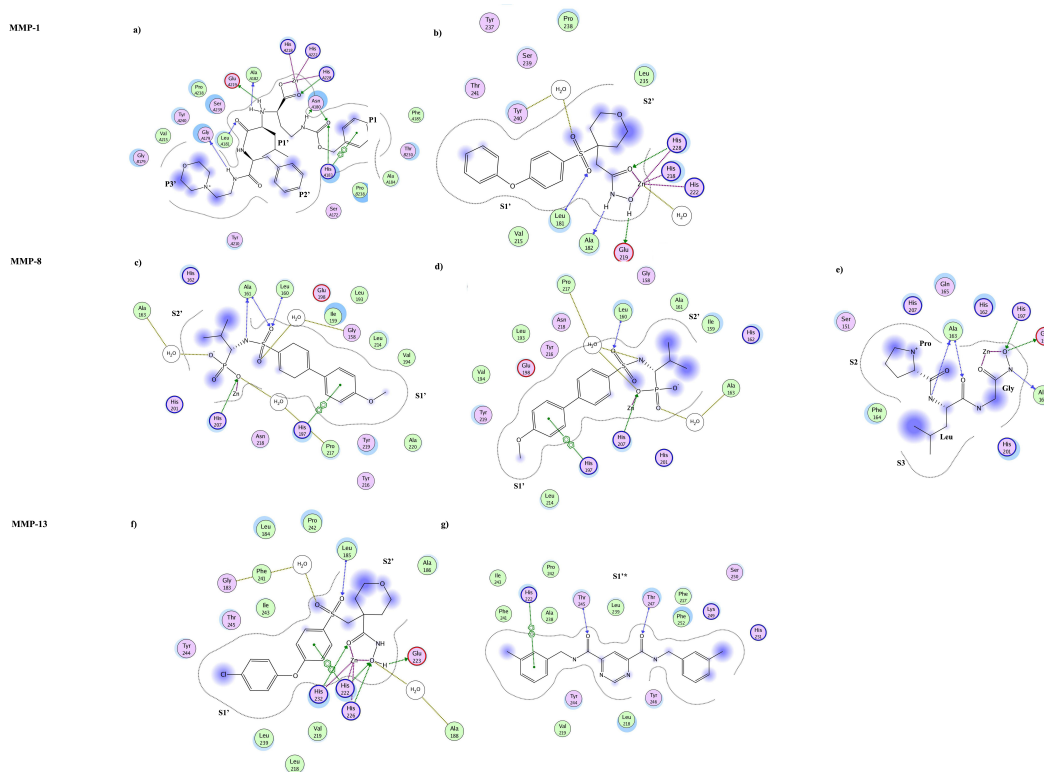


Fig. (3). Binding interaction diagrams for human collagenases: **MMP-1, MMP-8, MMP-13.**

Key residues involved in the inhibitor recognition are labeled. Blu (backbone) and green (side chain) dots show donors and acceptors hydrogen bonds, respectively; small green rings show π - π stacking interactions; light brown dots show the solvent contact; pink dots show the chelation of the catalytic Zn^{2+} ; blu areas show the ligand exposure to the solvent. All snapshots were made by using MOE tool [206].

Panel a, b: inhibitors (**1, 2**) complexed with CdMMP-1 (PDB code: 1cgl, 966c respectively).

Panel c, d, e: inhibitors (**4, 5, 9**) bound to CdMMP-8 (PDB code: 1zvx, 1zs0, 1jap respectively). **Panel c, d:** inhibitor (**4, -R**) is more efficient than (**5, -S**) for an additional hydrogen bond between its N-amide group and Ala¹⁶¹ backbone residue. Hydrophobic interactions of the biphenyl systems of both inhibitors with the enzyme S₁' pocket are depicted.

Panel e: Pro-Leu-Gly (**9**) is bound into the left-hand side of the human CdMMP-8.

Panel f, g: inhibitors (**10, 11**) complexed with human CdMMP-13 (PDB code: 830c, 1xuc). (**10**) has the classic hydroxamic ZBG; inhibitor (**11**) is devoid of a ZBG moiety. Both panels show the principal domains of MMP-13: S₁', S₂', S₁'*.

MMP-1 it comes out that this domain exhibits a different fold, characterized by four units of four-stranded antiparallel β -sheet stabilised by a calcium cation [58].

2.2.2. MMP-8 (Collagenase-2)

Eighteen 3D structures are, to date, available for MMP-8, as reported in Table (1A) [62-75].

The main difference between the MMP-1 and MMP-8 S₁' binding pocket is the large opening observed in the latter one (formed by residues Leu¹⁶⁰ and Ala¹⁶¹), while in MMP-1 S₁' is significantly occluded by the bulkier Arg²¹⁴. Therefore, specific P₁' groups should be taken into consideration for the design of inhibitors discriminating MMP-1 from MMP-8 [46, 66].

The crystal structure of the hMMP-8 complexed with both R- and S-enantiomers of sulfonamide phosphonates in-

hibitors (**4** and **5** in Table 2) is available at a resolution of 1.60 Å and 1.90 Å respectively (1zvx.pdb and 1zs0.pdb) [62]. Inspection of their 3D structure indicates that phosphonate acts as a favorable ZBG (Fig. (3c) and (3d)); thus, the stereoselective inhibition of MMP-8 by the enantiomeric sulfonamide phosphonates is particularly marked, the R- enantiomer (**4** in Table 2) showing a much higher inhibitory activity than the S- enantiomer (**5** in Table 2). This feature may be related to: (i) stronger H-bonds with the Ala¹⁶¹ backbone at the catalytic cleft; (ii) better and energetically more favorable hydrophobic interactions with Pro²¹⁷, Tyr²¹⁸, Tyr²¹⁹, Ala²⁷⁰, Val¹⁹⁴, Leu²¹⁴ and Ile¹⁵⁹ at the S₁' subsite; (iii) π -stacking with His¹⁹⁷.

Another interesting 3D structure is the CdMMP-8 complexed with a tetrahydroisoquinoline-3-carboxylate inhibitor (**6** in Table 2) solved at 1.7 Å resolution (1bzs.pdb) [63]. The

inspection of this structure illustrates how the loss of the inhibitory efficacy due to a weak ZBG, such as the carboxylate, can be compensated by an optimal fit of the P₁' biphenyl system into the S₁' pocket.

Interestingly, the crystal structure of the MMP-8 catalytic domain complexed with a barbituric acid (**7** in Table 2), solved at 2.0 Å (1ij9.pdb), reveals a previously unobserved ligand recognition mode [64]. In fact, the barbituric acid chelates the catalytic Zn²⁺ ion through the 2-hydroxyl group and the N₃ atom and rigidly orients its two cyclic substituents into the S₁' and S₂' sites. A conformational rearrangement accompanying this binding geometry occurs near the catalytic zinc, with a major contribution from the repulsive interaction between the barbiturate C₄=O₄ keto group and the Pro²¹⁷ carbonyl group [64]. The inhibitor binding induces a 0.6 Å shift of the catalytic Zn²⁺ ion, of the side chains of the three coordinating His residues and of the catalytic Glu¹⁹⁸. This displacement results from the optimization of the chelation geometry and leads to a new and highly ordered crystal packing [64]. In addition, MMP-8 shows a peculiar structural arrangement of the Asn¹⁸⁸ and Tyr¹⁸⁹ residues (located at the corridor connecting the catalytic and the C-terminal domain), which adopt a *cis*-peptide bond, with possible consequences for the substrate recognition process [64].

Finally, we have selected two examples of inhibitors bound into the left-hand side (unprimed region) of MMP-8. The first one is the hMMP-8 catalytic domain complexed with the hydroxamate inhibitor Batimastat (**8** in Table 2) refined at 2.1 Å (1mmb.pdb) [65]. This structure demonstrates that Batimastat binds from the S₁ left site to S₂' pocket and coordinates the catalytic zinc in the classical bidentate manner *via* the hydroxyl and carbonyl oxygens of the hydroxamate group [65]. The second example is the hMMP-8 catalytic domain bound to Pro – Leu – Gly hydroxylamine inhibitor (**9** in Table 2) solved at 1.80 Å (1jap.pdb) [66]. This left-hand side inhibitor sits in a large shallow S₂ subsite and in an invaginated S₃ subsite (Fig. (3e)), which could well accommodate the P₂ and P₃ groups (Pro–Leu) of this inhibitor [66].

2.2.3. MMP-13 (Collagenase-3)

To date, fifteen 3D structures of MMP-13 have been solved, see Table (1A and B). [52,76-84].

Since MMP-13 is not expressed in the majority of human adult tissues under normal conditions and its overexpression is often associated to pathological processes its selective inhibition could be a very promising therapeutical goal for several diseases, including arthritis, osteoarthritis, degenerative disorders and cancer [85-87].

The MMP-13 S₁' pocket is a long and open channel able to easily accommodate large P₁' groups [52]. The contour of this tunnel is dominated by Leu²¹⁸ and by the conformation of the residues 244-255, which render the S₁' site larger than in other MMPs, forming the so called "S₁'* specificity loop". On the other hand, the S₃ pocket of MMP-13 is small and hydrophobic, due to the presence of the residues Tyr¹⁵⁵ and Phe¹⁶⁸. These residues bring about a restriction of the pocket size, as compared to other MMPs, such as MMP-12, MT-MMPs, MMP-7 and MMP-9 [59].

The catalytic domain of the hMMP-13 complexed with a sulphone hydroxamic acid inhibitor (**10** in Table 2) at 1.6 Å resolution is deposited (830c.pdb) [52]. The binding mode of compound (**10**), as shown in Fig. (3f), involves: (i) the Zn²⁺ ion chelation by the most common hydroxamic moiety; (ii) an hydrogen bond between the sulphonyl oxygen and the residue Leu¹⁸⁵; (iii) hydrophobic interactions between the aromatic system of the inhibitor and Leu²¹⁸, Val²¹⁹, Leu²³⁹, Ile²⁴³, Tyr²⁴⁴, Tyr²⁴⁵ residues at S₁' pocket; (iv), the tetrahydropyran ring points to the exposed solvent S₂' pocket.

The design of selective MMP-13 inhibitors with incorporated large P₁' groups has been mostly addressed to take advantage of the long and open S₁' pocket [52]. The observed selectivity of the diphenyl ether series toward MMP-13 is due to their affinity to the preformed S₁' pocket. Thus, the larger size of the S₁' pocket (enriched by the S₁'* specificity loop) increases the affinity of bulky ligands for MMP-13 with respect to other MMPs, such as MMP-1, where the smaller S₁' pocket requires an induced-fit process to accommodate the inhibitor molecule into the pocket, decreasing the affinity [52]. An example of this *rationale* is represented by a novel class of selective pyrimidine dicarboxamide MMP-13 inhibitors, which are characterized by a nanomolar inhibitory activity not detected for other MMPs [76,77,88]. These compounds show a non-competitive inhibition mechanism with respect to substrate binding, also displaying an extreme selectivity for inhibiting MMP-13 *via* a non chelating process [76,77,88]. In the non-competitive inhibition, the inhibitor and the substrate bind independently and simultaneously to the enzyme at non-overlapping sites, and the inhibitor binds with the same affinity to the free enzyme and to the enzyme-substrate complex [77]. The presence of the bound substrate does not alter the inhibitor binding affinity and *viceversa* (keeping K_m unchanged). In this case, the inhibition is due to the fact that the inhibitor-bound enzyme displays a slow rate-limiting catalytic constant (i.e., k_{cat}) [77].

The crystal structures of these enzyme/inhibitor complexes reveal a new binding mode characterised by the absence of interaction between the inhibitors and the catalytic zinc (1xuc.pdb, 1xud.pdb, 1xur.pdb, 2ow9.pdb, 2ozr.pdb); the inhibitor structures are shown in Table 2 (**11**, **12**, **13**, **14**, **15** respectively) [76, 77]. The inhibitory strength and the target specificity can be explained by the perfect complementarity of these inhibitors with the S₁'* specificity loop (formed by residues 244-255, see above). These inhibitors deeply bind in the S₁' pocket, where they interact through a network of hydrogen bond with residues Thr²⁴⁵ and Thr²⁴⁷, extending their interaction into the S₁'* specificity loop. The binding mode and orientation of compound (**11**) into the catalytic cleft of MMP-13 is depicted in Fig. (3g). Interestingly, the catalytic Zn²⁺ ion is at about 6 Å from the binding site of this inhibitor.

Structural data suggest that the nature of the residues at position 218 (Leu) and 248 (Gly), as well as the sequence and conformation of this S₁'* specificity loop at the bottom of the S₁' pocket, are critical determinants for the selective inhibition [76,77,88,89]. In the complexes of MMP-13 with these inhibitors, the ordered structure of the specificity loop is conferred by the Gly²⁴⁸ residue, which allows the formation of an optimal hydrogen bonding geometry with residues

Thr²⁴⁵ and Thr²⁴⁷. This is a crucial aspect of recognition, since in other MMPs, where this loop is instead very flexible, the ligand binding turns out to be energetically unfavourable [76,77,88,89].

The sequence alignment reveals that the specificity loop in MMP-1, MMP-2 and MMP-9 is too short to accommodate this class of inhibitors, since a shorter loop makes the S'₁ pocket too shallow in MMP-1 and too narrow in MMP-2 and MMP-9. On the other hand, the S'₁ specificity loops in MMP-3 and MMP-17 is longer than in MMP-13, increasing its flexibility and accounting for the lack of detectable inhibition in these MMPs by such inhibitors (**11,12,13,14,15** in Table 2) [77].

On the other hand, MMP-8, MMP-12 and MMP-14, although displaying the same length for the specificity loop as compared to MMP-13, show a larger S'₁ pocket and some non-Gly residues in energetically unfavourable conformations at the key position 248. This is enough to impair the interaction of these inhibitors (**11,12,13,14,15** in Table 2) with such classes of MMP [77].

Moreover, the X-ray structures show that the residue Leu²¹⁸ is also critical for the formation of the complexes. Thus, MMP-1, MMP-7 and MMP-11, which contain bulkier residues at the same position (i.e., Arg or Tyr), show an unfavourable access to the S'₁ pocket with a consequent decrease of the inhibitor affinity [77].

The structure of the catalytic domain of mouse MMP-13 complexed with a hydroxamic acid inhibitor (**16** in Table 2) has been determined at 2.0 Å resolution (1cxv.pdb in Table 1B) [84]. The binding mode is superimposable to that already described in the literature for the sulfonamide hydroxamic acid series [84]. Like human MMP-13, the murine enzyme has a deep hydrophobic S'₁ pocket with no boundary at the bottom [84].

As a whole, different collagenases seem to exploit the different conformation and size of the S'₁ pocket to discriminate among substrates (and thus inhibitors), such that MMP-1 prefers smaller P'₁ groups, while MMP-13 is able to interact efficiently also with larger and extended P'₁ groups. On the other hand, MMP-8 seems to possess a wide number of recognition pockets, including both the S'₂ pocket (formed by residues Pro²¹⁷, Asn²¹⁸ and Tyr²¹⁹) and an even farther site represented by the *cis*-peptide bond between Asn¹⁸⁸ and Tyr¹⁸⁹ [64].

2.3. Gelatinases

The gelatinase family comprises MMP-2 and MMP-9. MMP-2 is a constitutively synthesized protein, activated by membrane-type MMPs, such as MMP-14. On the other hand, MMP-9 is mainly produced by inflammatory cells and it is activated by MMP-3 and by plasmin; the MMP-9 expression is highly regulated, as compared to that of MMP-2 [90,91].

The structures of MMP-2 and MMP-9 show highly homologous catalytic domains (both characterized by the insertion of the fibronectin-like module), but a different topological relationship between the catalytic domain and the haemopexin-like C-terminal domain. In fact, while in MMP-2 these two domains are separated by a short linker region

(similar to collagenases, see paragraph 2.2), in MMP-9 the catalytic domain and the haemopexin-like domain are separated by a long highly glycosylated collagen V-like domain [92].

Although the two enzymes show similar profiles for substrate recognition, a few differences occur in the S'₁ pocket, indeed the geometry of the 425-431 loop of MMP-9 is different from that of MMP-2 [44,93].

Interestingly, the S'₂ site contains the main differences between the two gelatinases: Glu⁴¹² of MMP-2 is replaced by Asp⁴¹⁰ in MMP-9 [94], bringing about a significant reduction of MMP-9 catalytic activity. This effect is related to the fact that while Glu⁴¹² of MMP-2 forms one hydrogen bond with the backbone of the selective substrate, this cannot be realised in MMP-9, since Asp⁴¹⁰ cannot protrude into the cleft enough to form the H-bond [94]. These residues are highly variable in other MMPs, where they are replaced by either large hydrophobic residues or by a small glycine, providing an important structural element for substrate recognition across the MMP family [94].

Moreover, the S'₃ pocket, which shows a high variability among different MMPs (e.g., at position 193 Tyr occurs in MMP-2, stromelysins and MMP-12, Asn in MT-MMPs, Ile in MMP-7 and Gln in MMP-9), is smaller in the gelatinase subfamily with respect to other MMPs. This structural information indeed could be relevant for designing selective and innovative MMP-2 inhibitors [95].

As a whole, it comes out that the substrate recognition by gelatinases is modulated by multiple specificity pockets, which extend from the unprimed S'₂ (on the left-hand side of the catalytic site) to the S'₃ specificity pocket, underlying a much wider interacting surface [94,95].

2.3.1. MMP-2 (Gelatinase A)

Seven 3D structures of MMP-2 have been to date deposited at the RCSB PDB, see Table (1A) [92,96-100].

The crystal structure of the full-length hproMMP-2 is reported at 2.08 Å resolution (1ck7.pdb) [92]. The inspection of the 3D structure indicates that the propeptide forms a globular domain, characterised by a three-helix fold, which is stabilised by hydrophobic and hydrogen bonds (Fig. (1)). MMP-14 activates proMMP-2 by cleaving the loop between α -helices H1 and H2, which contains a disulfide bridge (Cys⁶⁰ to Cys⁶⁵) that is unique to proMMP-2 [92]. A second loop (between Phe⁸¹ and Ile⁹⁴), stabilised by two internal hydrogen bonds, is also cleaved upon autoproteolytic activation; this process decreases the stability of the proenzyme, since this second loop contains hydrophobic side chains that isolate the catalytic cleft and the "Cys-switch" strand from the solvent. These loops within the propeptide domain act as a bait for the activating protease, since during the activation cleavage the prodomain structure breaks down, allowing water to enter and to hydrolyse the coordination of the Zn²⁺ ion to the Cys residue. Therefore, it might be of interest to test compounds which mimic the inhibitory activity of these two loops, impairing the access of the substrate to the catalytic Zn²⁺ ion [92].

In the full-length MMP-2 a likely important role is also played by the haemopexin-like domain, which contributes to

the formation of a groove that could be involved in the substrate binding.

Crystals of the C-terminal haemopexin-like domain of hMMP-2 have been solved by X-ray at 2.01 Å and 2.06 Å resolution (1gen.pdb and 1rtg.pdb respectively), showing that this domain has a disc-like shape [96,97]. Although the topology and the side-chain arrangement of the haemopexin-like domain of MMP-2 are very similar to the equivalent domain of fibroblast collagenase, significant differences in surface charge and contouring are observable, which might be responsible for the tendency of the MMP-2 C-terminal domain to bind selectively the natural inhibitor TIMP-2. The 3D structure of the MMP-2/TIMP-2 complex, which is very important for triggering the MMP-14-connected activation of proMMP-2, has been determined (see paragraph 3.2).

The 3D structure of CdMMP-2 in complex with a sulfonamide hydroxamic acid inhibitor (**17** in Table 2) has been determined by NMR spectroscopy (1hov.pdb) [98]; the binding mode of compound (**17**) is reported in Figs. (4a) and Fig. (5a). This structure indicates that the global fold of the CdMMP-2 (i.e., five-stranded β -sheets and three α -helices) closely resembles that observed in the full-length MMP-2, clearly indicating that the truncation of the haemopexin-like domain does not bring about a relevant perturbation of the active site [98]. Looking into more details, it becomes evident (Figs. (4a) and Fig. (5a)) that in MMP-2 the S_1' pocket is mainly hydrophobic for the presence of the side-chains of residues Leu⁸³, Phe¹¹⁵, Leu¹¹⁶, Val¹¹⁷, Leu¹³⁷ and Ile¹⁴¹ [98].

The same sulfonamide hydroxamic acid inhibitor (**17** in Table 2) has been also solved in complex with the CdMMP-8 and the comparative visual inspection shows some interesting differences with respect to MMP-2 [101]. Thus, the inhibitor is mostly recognized by the S_1' loop sequence, which is two residues shorter in MMP-2 than in MMP-8; this geometrical difference, associated to the hydrophobic interactions between the alkyl side chains of the P_1' moiety and the S_1' pocket accounts for the higher inhibitor affinity observed for MMP-2 with respect to MMP-8 [98].

However, the comparison of the solution and the crystallographic structure of MMP-2 demonstrates that several aromatic residues exhibit significant differences in their side-chain positions. Thus, the side chains of Phe⁶⁵ and Phe⁷⁶ point to the solvent in the solution structure, while they are buried in the internal pocket in the crystal structure [98]. Moreover, significant differences occur in the side-chain locations of Phe¹⁴⁸ and Arg¹⁴⁹, since in the crystal structure the side-chain of Phe¹⁴⁸ points into the active site and that of Arg¹⁴⁹ protrudes into the solvent. On the other hand, in the solution structure the Phe¹⁴⁸ aromatic ring has moved toward the protein surface to avoid van der Waals conflict with the inhibitor and the Arg¹⁴⁹ side-chain is rotated to compensate the movement of Phe¹⁴⁸ [98].

2.3.2. MMP-9 (Gelatinase B)

The query "MMP-9" in the RCSB databank has produced nine answers (see Table 1A) [93,102-104].

MMP-9 adopts the typical MMP fold, where the catalytic center is composed of the Zn²⁺ ion co-ordinated by three His residues and by the Glu side chain [93].

The X-ray crystal structure of hproMMP-9 (C-terminally truncated) has been solved at 2.5 Å resolution (116j.pdb) [102], showing that the prodomain, inserted into the active-site cleft, blocks the access to the catalytic zinc. The prodomains of MMP-9 and MMP-2 are identical in terms of placement of the "Cys-switch" peptide in the active site, even though the N-terminus of the propeptide has a slightly different conformation in MMP-2. However, the linker region between the propeptide and the catalytic domain (Gly¹⁰⁵ - Leu¹¹⁴) has a different conformation in the two MMPs [102].

The C-terminal haemopexin-like domain of MMP-9 has been deposited and solved at 1.95 Å (1itv.pdb) [103]. This domain plays a major role in regulating MMP activation, recognition and inhibition by binding different regulatory proteins. A dimeric structure has been proposed for the haemopexin-like domain of MMP-9, due to intermolecular disulfide bonds that could generate peculiar physico-chemical and functional properties [103].

The X-ray structures of hMMP-9 with five different classes of inhibitors (**18,19,20,21** and **22** in Table 2) have been recently determined (2ovx.pdb, 2ovz.pdb, 2ow0.pdb, 2ow1.pdb, 2ow2.pdb) [104]. The binding mode, as shown in Fig. (4b) and Fig. (5b), in general shows: (i) an optimal coordination of the catalytic zinc, (ii) a favourable hydrogen bonding in the active-site cleft and (iii) an accommodation of the inhibitors hydrophobic P_1' groups in the slightly flexible S_1' cavity of MMP-9.

In both MMP-2 and MMP-9 the S_1' pocket is larger than in other MMPs. Further, in all these selected complexes, the side chain of Arg⁴²⁴, located at the bottom of the S_1' pocket, adopts different conformations. This behaviour is connected to the flexibility of the Arg⁴²⁴ side-chain in MMP-9, which partially blocks the S_1' cavity, preventing the binding of most of the inhibitors with long P_1' groups. Moreover, the side chain of Arg⁴²⁴ in MMP-9 is slightly more angled away from the S_1' pocket than the corresponding residue Thr⁴²⁴ in MMP-2; this represents the main (though small) difference between the S_1' binding pockets of MMP-9 and MMP-2. These structural details should be taken into account for designing specific inhibitors discriminating between the two gelatinases [93,104].

2.4. Stromelysins

Many 3D structures with a large variety of inhibitors are available for the catalytic domain of stromelysin-1 (MMP-3) [78, 105-124]. Conversely, only one X-ray structure is reported, respectively, for stromelysin-2 (MMP-10) and stromelysin-3 (MMP-11) [125,126]. All these complexes are listed in Table (1A and B).

2.4.1. MMP-3 (Stromelysin-1)

The three-dimensional structure of the C-truncated proMMP-3 was determined by X-ray diffraction analysis at 1.9 Å resolution (1slm.pdb), showing a structure of the proenzyme catalytic domain remarkably similar to that of the active enzyme [105]. The pro-domain displays a separate folding characterised by three α -helices and an extended propeptide that occupies the active site blocking the catalytic Zn²⁺ ion. The active site consists of two distinct regions: a groove

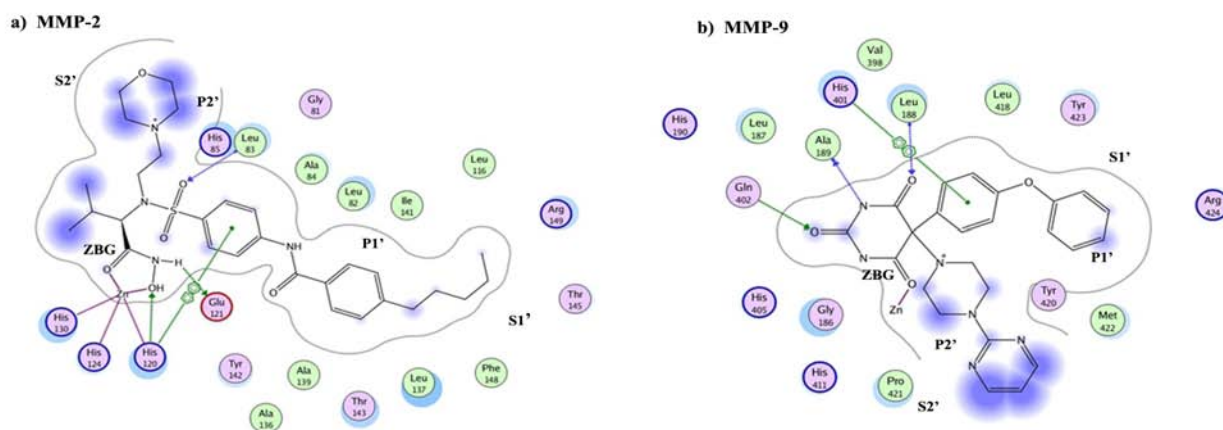


Fig. (4). Binding interaction diagrams for human gelatinases: **MMP-2**, **MMP-9**.

For symbols comprehension see legend of Fig. (2).

Panel a: inhibitor (**17**) complexed with CdMMP-2 (PDB code: 1hov). The alkyl-phenyl P₁' moiety fits deeply into the S₁' subsite, closed by Thr¹⁴³, through hydrophobic contacts.

Panel b: inhibitor (**18**) bound to CdMMP-9 (PDB code: 2ovx). ZBG is the barbiturate ring; P₁' is the *p*-phenoxy system that binds into the S₁' subsite, closed by Arg⁴²⁴.

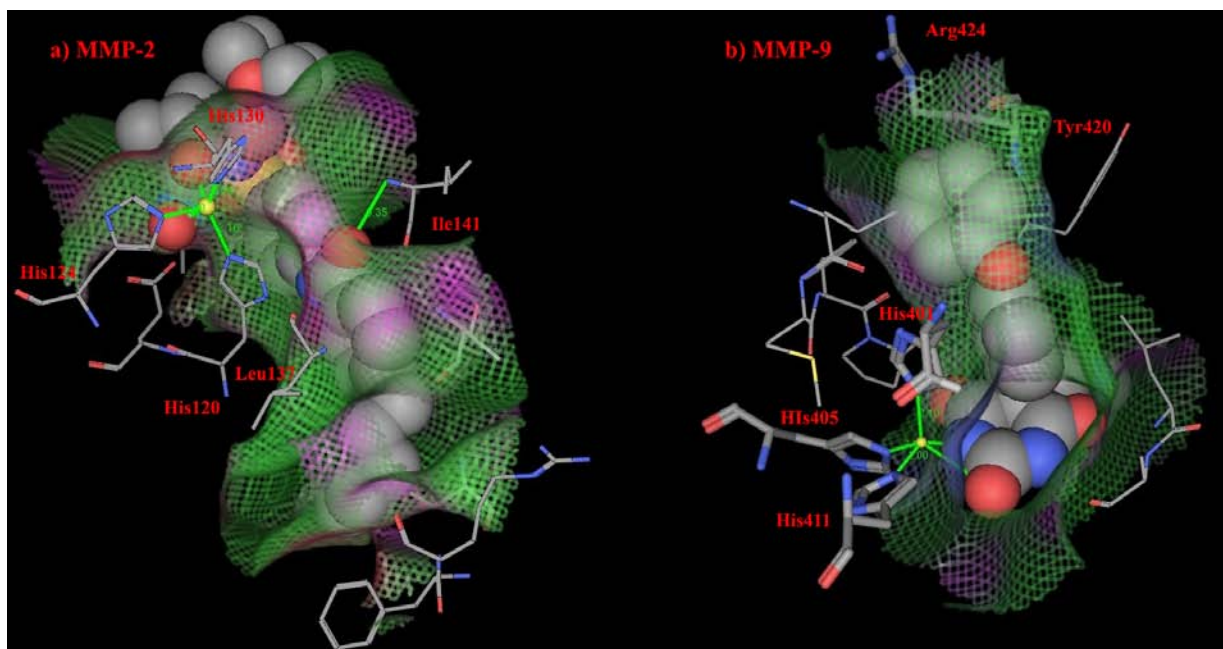


Fig. (5). 3D maps for inhibitors (**17**) and (**18**) co-crystallised with **MMP-2** and **MMP-9**, respectively.

The maps are coloured according to the inhibitors electrostatic properties: green refers to hydrophobic area; red to solvent exposed; violet to polar area. Key residues are labeled. Both pictures were made by using MOE tool [206].

Panel a: 3D map for inhibitor (**17**), using CPK representation, in MMP-2 binding site (PDB code: 1hov). The picture shows the MMP-2 long and hydrophobic S₁' channel.

Panel b: 3D map for inhibitor (**18**), using CPK representation, in MMP-9 binding site.

in the protein surface and a large predominantly hydrophobic S₁' pocket that extends throughout the full width of the catalytic domain [105]. In the proenzyme and in the active protein the groove is occupied by extended peptide chains that make several β -like structures.

The activation process involves a substantial rearrangement of residues 83-89 [105] (part of a large loop that

crosses the active site groove), which during the activation process move to a different position, forming a salt link between the nitrogen atom of Phe⁸³ and the side chain of Asp²³⁷ in the helix C. Therefore, when the active and the proenzyme structures of MMP-3 are superimposed, the respective residues in position 83 are more than 17 Å away from each other [105].

The catalytic domain of hMMP-3 complexed with a sulphonamide carboxylic acid inhibitor (**23** in Table 2) is described (Fig. (6a)) by X-ray analysis at 1.5 Å definition (1hy7.pdb) [106] and homology modeling [127]. The biphenyl moiety of this inhibitor fits into the S₁' pocket of the enzyme; the carboxylic acid binds the Zn²⁺ ion in the active site, while the alkylnyl side chain of the inhibitor prefers the lipophylic S₂ cleft [106]. Despite the fact that the inhibitor makes similar interactions with the pro-enzyme and the active enzyme, the N-to-C direction of the propeptide backbone is opposite of that adopted by the inhibitor bound to the active MMP-3 [105,106]. Thus, while the S₁' subsite is empty in the proenzyme structure, it contains the side chain of the phenylalanyl residue in the inhibited complex with active MMP-3 [105].

2.4.2. MMP-10 (*Stromelysin-2*)

MMP-3 and MMP-10 show the highest identity and sequence homology among all MMPs; however, small differences exist between their catalytic domains. The main difference consists in a loop that involves residues 240-247, indeed it is stabilised in a more rigid conformation in MMP-10, whereas MMP-3 shows higher conformation flexibility [125].

As expected from the high similarity in the catalytic domain, no differences affect MMP-10 and MMP-3 at level of the groove that hosts the substrate. However, molecular modeling studies suggest that the haemopexin domain contributes to the definition of the substrate-binding region [125]. The haemopexin-like domain shows a lower sequence identity (74%) between MMP-10 and MMP-3 and this should account for the selective modulation of the catalytic activity and of substrate recognition [125].

The crystal structure of the catalytic domain of hMMP-10, complexed with a hydroxamic acid chelating inhibitor (**24** in Table 2), has been solved at 2.1 Å resolution

(1q3a.pdb) [125]. The binding mode indicates that inhibition occurs *via* the Zn²⁺ chelation through the hydroxamic moiety and van der Waals contacts with residues His¹⁷⁸, Leu²¹⁸, Pro²³⁷ at the S₁' and S₂' pockets of MMP-10 (Fig. (6b)).

2.4.3. MMP-11 (*Stromelysin-3*)

Differently from other MMPs, MMP-11 is secreted already as an active enzyme and its substrates have not been characterised yet. MMP-11 could play a unique role in tissue remodeling processes, including those associated with tumor progression [128].

The crystal structure of the mouse MMP-11 catalytic domain, complexed with a phosphinic inhibitor (**25** in Table 2), has been solved at 2.6 Å resolution (1hv5.pdb in Table 1B) [126]. The inspection of the 3D structure (Fig. (6c)) clearly indicates that the S₁' pocket corresponds to a deep open tunnel running through the enzyme matrix, such that the P₁' group of the inhibitor must adopt a constrained conformation to fit into the S₁' pocket. The inhibitor interacts with the enzyme through several hydrogen bonds like a peptidic substrate, mimicking the tetrahedral geometry of a scis-side peptide bond during enzymatic hydrolysis. It is worth outlining that the phosphinic peptide chemistry offers the possibility to develop inhibitors which are able to interact with both primed and unprimed sides of the active site cleft [126,128].

2.5. Matrilysins

To date four 3D structures have been solved for Matrilysin (MMP-7) (see Table 1A) [32,129].

MMP-7 is the smallest member of the MMPs family, since it completely misses the haemopexin-like domain. The X-ray crystal structures of hMMP-7 complexed with hydroxamate, carboxylate and sulfodiimine inhibitors (**26**, **27** and **28** in Table 2, respectively) have been published (1mmq.pdb, 1mmp.pdb, 1mmr.pdb, respectively) [129]. In this series of

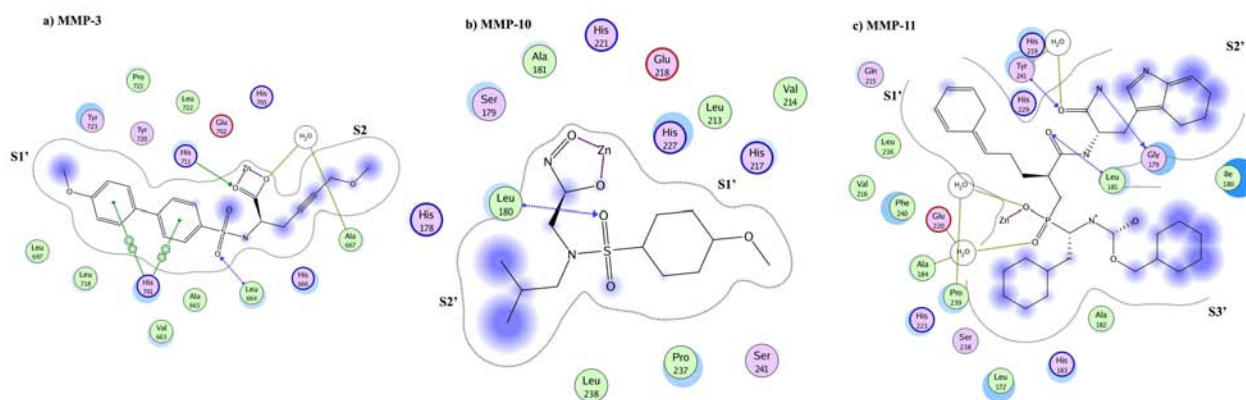


Fig. (6). Binding interaction diagrams for stromelysins: **MMP-3**, **MMP-10**, **MMP-11**.

For symbols comprehension see legend of Fig. (2).

Panel a: inhibitor (**23**) complexed with CdMMP-3 (PDB code: 1hy7). ZBG is the carboxylic acid; the biphenyl P₁' moiety fits into the S₁' pocket; the alkylnyl side chain prefers the S₂ pocket.

Panel b: inhibitor (**24**) bound to CdMMP-10 (PDB code: 1q3a). ZBG is the hydroxamic acid; P₁' is the aromatic ring; P₂' is the isopropyl chain.

Panel c: inhibitor (**25**) bound to murine CdMMP-11 (PDB code: 1hv5). ZBG is a phosphinic moiety; the inhibitor mimicks the peptidic substrate showing several hydrogen bonds with the target.

inhibitors, the only variation concerns the group coordinating the Zn^{2+} ion. These structures provide detailed information on how each functional group interacts with the catalytic zinc, representing a structural basis for comparing MMP-7 with other MMPs [129]. In Fig. (7a) the binding mode of the sulfodiimine inhibitor (**28** in Table 2) to the MMP-7 binding site is depicted, showing that (i) the sulfodiimine group chelates the catalytic zinc ion, (ii) the alkyl group interacts with the S'_1 pocket, and (iii) the cyclic system points to the S_2 pocket.

The MMP-7 fold is an open-face α - β sandwich very similar to that reported for other MMPs, however its S'_1 pocket is much smaller than that of MMP-1. Thus, the flexibility of the MMP-1 Arg²¹⁴ residue at the bottom renders the S'_1 pocket able to accommodate larger substituents, whereas the Tyr²¹⁴ residue of MMP-7 at the same position induces a more rigid S'_1 pocket conformation, allowing the access only to smaller inhibitors. Further, while MMP-1 is able to adapt its shape and to accommodate more bulky substituents, the rigidity of the MMP-7 S'_1 pocket is not affected by the induced-fit mechanism upon inhibitor binding [129].

Similarly to MMP-7, two other MMPs (namely MMP-23 and MMP-26) lack the C-terminal haemopexin-like domain [39]. Interestingly, the MMP-23 gene has been isolated from gonadotropin-primed immature rat ovaries in order to study the role of this isoform in the mammalian ovulation process [130].

Human matrilysin-2 (MMP-26) is a recently discovered epithelial MMP which is highly expressed in several cancer cell lines [131]; a model of proMMP-26, built by computer modeling using MMP-3 as template, has also been determined (1slm.pdb) [132]. The biological function and the substrate specificity of MMP-26 are not fully understood yet. ProMMP-26 presents a “Cys-switch” motif (Pro-His⁸¹-Cys-Gly-Xxx-Xxx-Asp) that discriminates this protease from all other MMPs known to date, indeed this sequence is not func-

tional and is not involved in the activation mechanism. Computer modeling studies indicate that His⁸¹ significantly modifies the fold of proMMP-26, abolishing the functionality of the “Cys-switch” motif and inducing an alternative intramolecular activation pathway of the proenzyme [132].

2.6. Membrane Type MMPs

Five membrane-type MT-MMPs (MMP-14, -15, -16, -17 and MMP-24) have been described and represent very promising potential targets for therapeutic applications [41,133-136]. Thus, MT1-MMP (i.e., MMP-14), MT2-MMP (i.e., MMP-15), MT3-MMP (i.e., MMP-16), MT4-MMP (i.e., MMP-17), MT5-MMP (i.e., MMP-24) play a key role in the cell surface proteolysis, being able to cleave a variety of extracellular matrix components [41, 133-136]. While MMP-14 and MMP-15 are expressed in a variety of adult human tissues, the expression of MMP-16 and MMP-24 seems to be restricted, under normal conditions, to the brain and the heart respectively [137].

MMP-14 is the major activator of proMMP-2 *via* presentation of proMMP-2 to a MMP-14-TIMP-2 “receptor” [133] and the structure of the complex between human MMP-14 and bovine TIMP-2 has been described (see below). The proMMP-2 activation ability has been associated to a characteristic loop insertion of MMP-14, not present in MMP-17 and MMP-24, which in fact are not able to promote an activation mechanism [138, 139]. On the other hand, MMP-15 is able to perform this activation, but in a TIMP-2 independent manner [138]. MMP-14 differs from other MMPs for the hydrophobic nature of the S_2' pocket due the presence of the Phe¹⁹⁸ residue. Furthermore, the S'_1 pocket of MMP-14 is characterized by a reduced size due to the presence of Phe¹⁶³ and Met²³⁷ at the cleft bottom [59].

MMP-16 (MT3-MMP), like related MT-MMPs, is expressed as a multidomain 607-residue polypeptide chain, consisting of: (i) a short signal peptide, (ii) a prodomain

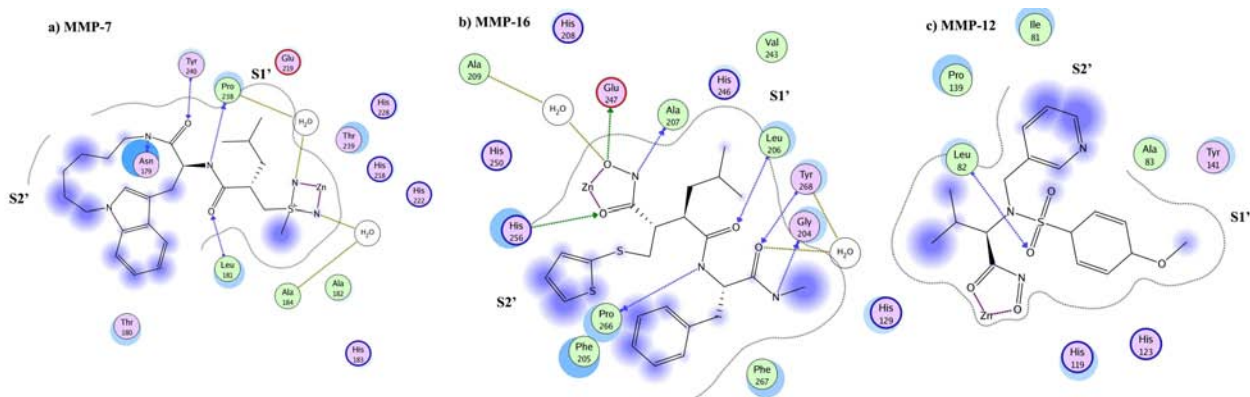


Fig. (7). Binding interaction diagrams for: **MMP-7**, **MMP-16**, **MMP-12**.

For symbols comprehension see legend of Fig. (2).

Panel a: inhibitor (**28**) complexed with CdMMP-7 (PDB code: 1mmr). ZBG is a sulfodiimine group; P'_1 is a alkyl chain; P'_2 is a cyclic system.

Panel b: Batimastat (**8**) complexed with human CdMMP-16 (PDB code: 1rm8). Batimastat coordinates the catalytic Zn^{2+} in a bidentate bipyramidal manner, through its hydroxamic ZBG.

Panel c: inhibitor (**29**) complexed with CdMMP-12 (PDB code: 1jiz). ZBG is the classic hydroxamic function; while the aromatic systems are both positioned into S'_1 and S'_2 pockets.

linked *via* a multiple basic furin cleavage site to the catalytic domain, (iii) a long linker, (iv) a haemopexin-like domain, (v) a transmembrane helix, (vi) a short cytoplasmatic tail [136]. According to the topology-based sequence alignment, the sequence of residues forming the catalytic domain of MMP-16 (Tyr¹²⁰ - Gly²⁹¹) is 68 % identical to that of MMP-14 and 80% identical to that of MMP-24 [137]. The structure of the MMP-16 catalytic domain has been solved in the presence of the Batimastat inhibitor (1rm8.pdb) (**8** in Table 2), which coordinates the catalytic zinc in a bidentate bipyramidal manner [136] (Fig. (7b)). The catalytic domain of MMP-16 exhibits a classical MMP fold closely similar to that of MMP-14 and their active site clefts indeed are similar [136]. Thus, both MMP-14 and MMP-16 are inhibited by TIMP-2 but not by TIMP-1 [136]. Nevertheless, MMP-16 also shows unique properties, which could help in the rational design of selective inhibitors, such as a modified MT-specific loop and a closed S₁ specificity pocket [136].

Finally, the human form of MT4-MMP (MMP-17) and MT5-MMP (MMP-24) have also been identified [134,135].

2.7. MMP-12 (Metalloelastase)

To date, fifteen 3D structures have been solved for macrophage MMP-12, as reported in Table (1A) [140-147].

MMP-12 adopts the typical MMP fold and binds a structural Zn²⁺ and three Ca²⁺ ions in addition to the catalytic Zn²⁺ ion [140]. The enzyme structure shows an ordered N-terminus close to the active site; moreover the S₁ pocket is large and extends to a channel through the protein matrix. According to the S₁ pocket shape, MMP-12 is normally classified within MMPs displaying a large and open S₁ pocket, a group which also includes MMP-3, MMP-8 and MMP-13 [140]. In addition, the conformation of MMP-12 S₁ loop is very similar to that of MMP-8, since both enzymes exhibit one helical turn at residues Asp²⁴⁴ - Phe²⁴⁸ (MMP-12 sequence numbers) at the bottom end of the S₁ subsite [140]. On the other hand, while the MMP-8 S₁ subsite is closed by the presence of the Arg²¹⁴ residue, the MMP-12 S₁ pocket is more open and extends by a channel through the protein surface. In addition, the residue Thr²¹⁵, which is usually replaced by Val or Ala in the majority of MMPs, is observed at the wall of the MMP-12 S₁ pocket, providing the basis for a selective and favourable interaction with polar binding groups [140].

Moreover, MMP-12 can be clearly distinguished from other MMPs, since its S₂' pocket is extensively exposed to the solvent. Arg⁸⁴ and Met⁸⁶ residues are surrounding this pocket and both side chains are able to move freely, making the recognition cleft very wide and flexible [59].

Crystal structures of hMMP-12 catalytic domain with many Zn²⁺ ion-chelating inhibitors have been described (1jiz.pdb, 1y93.pdb, 1rmz.pdb, 1ycm, 1z3j in Table 1A); the inhibitor structures are shown in Table 2 (**29**, **30** and **31** respectively) [140,141]. In general, these inhibitors bind the catalytic zinc in a bidentate manner such that their polar groups form hydrogen bonds in a substrate-like manner, while the hydrophobic substituents are either positioned on the protein surface or inserted into the S₁ specificity pocket (Fig. (7c)) [140].

Recently, the NMR structure of hMMP-12 without inhibitors has been solved (2poj.pdb) [147]. Helix B at the active site is measurably deeper in this solution structure than in the crystal structure of MMP-12 (in the presence of inhibitors), making the active site an open channel. Conversely, the inhibitor-binding induces extensive conformational adjustments [147].

A new human epilysin (MMP-28) has been cloned and characterised [148,149], suggesting that this enzyme could represent an important functional target in some carcinomas. MMP-28 has a 520-aminoacid sequence including a signal peptide, a prodomain with the unusual "Cys-switch" motif (Pro-Arg-Cys-Gly-Val-Thr-Asp), a Zn²⁺ ion-binding catalytic domain, a hinge region and a haemopexin-like domain [149]. In addition, MMP-28 has the furin activation sequence (Arg-Arg-Lys-Lys-Arg) but has no transmembrane sequence [149].

3. MACROMOLECULAR INHIBITOR RECOGNITION BY MMPs

3.1. General Aspects

The proteolytic activity of MMPs is regulated under physiological conditions by endogenous tissue inhibitors (i.e. TIMPs) [35,150,151]. An unbalanced modulation of MMPs by TIMPs brings about diseases such as arthritis, atherosclerosis, tumor growth and metastasis diffusion [26,152,153]. Therefore, a careful balancing between MMPs and TIMPs is a crucial event, which is altered in many pathological processes [26,152,153]. Despite TIMPs were traditionally viewed as inhibitors, they have several additional functions, acting as growth factors, inhibiting the angiogenesis and taking part into the MMPs activation process [154]. The TIMP family comprises four members (TIMP-1 to TIMP-4) with 40-50% sequence identity [155]. All TIMPs inhibit active MMPs with relatively low selectivity, forming virtually tight non-covalent 1:1 complexes [156].

TIMPs structure is made of two domains, although only the N-terminal region (N-TIMP) has been shown to form a stable, autonomously folded unit. This domain includes three out of the six disulfide bonds and is able to form stable tight complexes with MMP catalytic domains [155,156]. The alignment of the amino acidic sequences of the representative TIMP families highlights the differences occurring mainly at the recognition loop region. Some of these differences have been proposed to be responsible for the selective inhibitory properties of TIMP [155,156].

The 3D structures of MMP/TIMP complexes provide a basis for designing TIMP variants with increased selectivity for different MMPs. Such variants are potentially useful to investigate the roles of different MMPs in biological and pathological processes and could provide new therapeutic strategies in diseases associated with an excess of the MMP activities [155]. Furthermore, MMP/TIMP 3D structures show an extended interaction surface for MMPs, giving a hint of additional recognition sites, spread over the whole macromolecule, which might be important for the inhibition of the enzymatic activity toward macromolecular substrates.

Fig. (7) shows the superimposition of the 3D structures of the MMP-3/TIMP-1 and MMP-13/TIMP-2 complexes.

The comparison highlights structural similarities among TIMPs, even though subtle differences may be noticed for MMP-TIMP interaction surfaces accounting for the inhibitory specificity (see below).

3.2. TIMP-1

TIMP-1 was originally discovered as a growth factor and the same activity was later demonstrated for TIMP-2 [157]. There is evidence that the growth factor activity is associated with the N-terminal domain and is independent from the physiological inhibitory properties of TIMPs. It has been proposed that TIMPs could interact with nucleic acids, accounting for their activity as growth factors, even though none of the TIMP disulfide bridges is conserved in DNA-binding proteins. Furthermore, the side chains, observed in human replication proteins and involved in DNA binding, are not conserved in TIMPs, making it unlikely that these two classes of protein may be related; the similarity of the overall structure is probably the result of a convergent evolution to a stable conformation [157].

A high quality solution structure of N-TIMP-1 (matrix metalloproteinase N-terminal domain human tissue inhibitor of metalloproteinases-1) has been determined (1d2b.pdb in Table 1A) [158]. The inspection of this structure indicates that the isolated N-terminal TIMP-1 (126 residues long) can independently fold and is sufficient to inhibit MMP-1 and MMP-3. Interestingly, although TIMP-1 has a similar affinity for MMP-1 and MMP-3, striking differences occur in the chemistry and in the structures of the interaction sites [158]. However, a comparison between the NMR solution structure

of free N-TIMP-1 and the CdMMP-3/TIMP-1 crystal complex shows that the structural core is nearly unchanged by the association with MMP-3 [158].

The availability of CdMMP-3/N-TIMP-1 complex (1uea.pdb in Table 1A) [159] allows the following considerations: (i) TIMP-1 (184-residues long) has the shape of an elongated and contiguous edge, which occupies the whole MMP-3 active site (Fig. (8)); (ii) the N-terminal segment Cys¹-Thr²-Cys³-Val⁴ binds the active site cleft (subsites S₁' to S₃'), positioning itself between two antiparallel β strands, where it makes further intermolecular contacts at the bottom of the MMP-3 cleft. In particular, Cys¹ is directly located above the catalytic zinc at a distance of about 2.0 Å and the central disulfide-linked segments bind on both sides of the catalytic zinc. Besides binding to the catalytic Zn²⁺ ion, the α -amino group (which is presumably unprotonated) could form hydrogen bonds with the neighbouring carbonyl oxygen atom of Ser⁶⁸ of TIMP-1 and with one of the carboxylate oxygen atoms of the catalytic Glu²⁰² residue of MMP-3; as a consequence, the side chain of Glu²⁰² moves closer to the Ser⁶⁸ side chain when TIMP is bound to the enzyme. This α -amino acyl group partially superimposes with the hydroxamic acid moiety, which commonly acts as a Zn²⁺ ion-chelating group in many synthetic MMP inhibitors [159].

The same orientation described for the complex MMP-3/TIMP-1 [159] has been confirmed using residual dipolar couplings in solution (1oo9.pdb) [160].

Moreover, the structure of the complex MMP-1/TIMP-1 (catalytic domain and human N-terminal inhibitory domain respectively) at a 2.54 Å resolution has been reported



Fig. (8). 3D superposition of the MMP-3/TIMP-1 and MMP-13/TIMP-2 complexes (PDB code: 1uea and 2ed2, respectively). MMP-3, green; TIMP-1, red; MMP-13, cyan; TIMP-2, orange. Both catalytic and structural Zn²⁺ ions are shown as spheres. The picture shows the homology of the 3D architecture of TIMP-1 and TIMP-2. The snapshot was made by PyMol software [205].

(2jot.pdb in Table 1A) [161]. Comparison of MMP-1/TIMP-1 and MMP-3/TIMP-1 complexes shows that the inhibition mechanisms of both MMPs are generally similar, even though significant differences for the protein-protein interfaces can be detected in the two complexes. In particular, beside several differences in the binding of individual residues of TIMP-1 with the two MMPs, the loop between β -strands A and B of TIMP-1 interacts with MMP-3 but not with MMP-1 [159,161].

3.3. TIMP-2

The three-dimensional structure of full length human tissue inhibitor of metalloproteinase-2 (TIMP-2) was determined by X-ray crystallography at 2.1 Å resolution (1br9.pdb in Table 1A) [162]. The structure of TIMP-2 consists of two domains, namely (i) the N-terminal domain (residues 1-110), which is folded into a β -barrel, resulting similar to the oligonucleotide/oligosaccharide binding (OB) protein fold found in some other DNA-binding proteins, and (ii) the C-terminal domain (residues 111-194), which contains a parallel stranded β -hairpin plus a β -loop- β motif. Comparison of the uncomplexed human TIMP-2 structure with that of bovine TIMP-2 complexed with the human CdMMP-14 unravels some global and local conformational changes occurring upon the formation of the proteinase-inhibitor complex; in particular, an internal rotation by $\sim 13^\circ$ within the two domains can be clearly observed [162].

The high NMR resolution of the human TIMP-2 N-terminal domain, which is 46 % identical with that of human N-TIMP-1, is available (2tmp.pdb in Table 1A) [163]. This information confirms that the core of the inhibitory domain is organized around a five-stranded β -barrel homologous to that found in the oligosaccharide/oligonucleotide binding protein fold. Furthermore, the β -hairpin in N-TIMP-2 is significantly longer than the equivalent structure in TIMP-1. This allows TIMP-2 to make more extensive binding interactions with the MMPs catalytic domain, not possible for TIMP-1 [163].

Finally, TIMP-2 is unique in that it can also bind to the pro-form of MMP-2 [164]. TIMP-2 is implicated in a unique cell surface activation mechanism of the latent proMMP-2, by binding the haemopexin-like domain of proMMP-2 on one side, and the MT1-MMP activator on the other one. The inspection of the 3D crystal structure of the hproMMP-2/TIMP-2 complex (1gxd.pdb in Table 1A) shows that the interaction between the proMMP-2 haemopexin-like domain and the C-terminal of TIMP-2 involves two distinct binding regions composed of alternating hydrophobic and hydrophilic clefts, leaving the catalytic site of MMP-2 and the inhibitory site of TIMP-2 spatially isolated [165]. The proMMP-2/TIMP-2 complex is localised on the cell surface and binds the active site of MT1-MMP, forming a ternary complex (i.e., proMMP-2/TIMP-2/MT1-MMP), which facilitates the activation of the proMMP-2 by another MT1-MMP molecule. The C-terminal tail of uncomplexed TIMP-2 is disordered but adopts a well defined structure upon binding to proMMP-2 [165].

Crystal structures of two complexes, formed by the catalytic domain of human MT1-MMP (i.e., MMP-14) and full

length bovine TIMP-2 at 2.75 Å resolution, have been solved (1bqq.pdb, 1buu.pdb in Table 1B) [139].

Superimposition of the CdMMP-3/TIMP-1 and the CdMT1-MMP/TIMP-2 complexes shows that both TIMPs undergo a considerable rotation at their interfaces with MMPs, even though different features are observed for the two complexes. For example, the CdMT1-MMP/TIMP-2 complex displays two large insertions, which are quite remote from the active site cleft and important for the interaction with substrates. Moreover, the Ser² side-chain of TIMP-2 extends into the wide S1' specificity pocket of MT1-MMP, interacting with the catalytic Glu²⁴⁰.

In addition, the crystal structure of the hMMP-13 catalytic domain complexed with a bovine TIMP-2 form, solved at 2.0 Å (2ed2.pdb in Table 1B), shows that TIMP-2 shapes on the specific MMP, its orientation depending on the specific proteinase [166]. Thus, after binding TIMP-2, the catalytic Zn²⁺ ion, the enclosing MMP loop and the S'₁ segment move significantly (Fig. (8)), allowing a more favourable interaction between the α -amino group of the Cys¹ residue of TIMP-2 and the catalytic Zn²⁺ ion of the enzyme [166].

As a whole, the very extended recognition surface between a given MMP and a specific TIMP (characterized by several widespread interactions) is a crucial determinant for the selective inhibitory action of TIMPs, as outlined by the observation that the affinity of MT1-MMP for TIMP-1 is lower than for TIMP-2 simply because of the reduced number of favourable interactions [139]. This evidence remarks the fact that the interactions of MMPs with macromolecular substrates (and/or inhibitors) involves a much larger portion of the molecule beside the active site, rendering the recognition process a much more complex event, where different domains play specific and important roles; this complexity should be taken into account for the design of selective synthetic inhibitors.

4. BIOINFORMATIC ANALYSIS AND HOMOLGY MODELS OF MMPs

The availability of the complete human genome sequence allowed to examine the whole family of human MMPs both in terms of phylogenetic trees and of 3D structural features [167]. The phylogenetic analysis has indicated that individual domains of each MMP have evolved in a correlated manner, showing a high degree of conservation of the catalytic domain around the active site cleft. The haemopexin-like domains result instead more variable in terms of surface shape and electrostatics profile; this suggests that they are important factors in modulating substrate specificity [167].

Homology modeling can be used to predict the 3D structures of proteins, whose three-dimensional structure has not been solved yet, taking advantage of structural information from known homologous proteins with similar amino acid sequence [168]. The comparative modeling is carried out using public sequence databases and algorithms, following a procedure, which can be summarized by: i) finding known structures (which are called template) related to the sequence to be modeled (which is called target); ii) aligning the target to the template sequence, iii) building the model, iv) assigning the modelled structure [168]. Clearly, the accuracy of the

built model depends on the degree of homology sequence between the target and the template proteins. The model is reliable if it is as accurate as a medium/low resolution X-ray structure, meaning that the error for the main-chain atoms can not be higher than 1 Å RMS [168].

Since MMPs are homologous enzymes, which share a high degree of sequence similarity and a conserved 3D organization, the homology modeling approach has been fruitfully used [169,170] and multiple sequence alignments have been successfully accomplished [168].

For this review we have performed a multiple-alignment for most representative MMP members taking MMP-1 (1hfc.pdb) as the template, by using CE algorithm [171]. From this approach it emerged that the 3D of catalytic do-

main of the most common MMPs exhibit the same folding and a high omology identity, resulting well superimposed. Values of parameters derived from the multiple-alignment approach are summarised in Table 3. The analysis of data reported in Table 3 indicates a high amino acid identity for most MMPs catalytic domains.

Several works regarding MMP homology modeling have been reported, especially for MMP-2, MMP-9, MMP-3, MMP-8, MMP-10, MMP-12, MMP-14, MMP-13, MMP-16, MMP-20 and MMP-26 [95,172-175]. Although several X-ray and/or NMR studies have been reported for most of these MMPs, homology modeling can still be useful to validate and eventually implement the structural information not available in the RCSB PDB databank (such as atomic informations and conformations) [168]. The application of this

Table 3. Multiple Alignment and Superimposition Parameters for MMPs

(A) Distance Matrix

	MMP-1	MMP-2	MMP-3	MMP-7	MMP-8	MMP-9	MMP-10	MMP-11	MMP-12	MMP-13	MMP-16
MMP-1	--	1.86	0.82	0.96	0.70	0.92	0.75	1.49	0.69	0.63	1.11
MMP-2		--	1.92	1.95	1.98	1.98	1.88	1.93	1.87	1.79	1.93
MMP-3			--	0.84	0.89	0.84	0.57	1.67	0.75	0.57	1.23
MMP-7				--	1.07	1.19	0.95	1.72	1.35	1.08	1.31
MMP-8					--	1.01	0.81	1.63	0.71	0.63	1.02
MMP-9						--	0.95	1.61	0.77	0.77	1.16
MMP-10							--	1.71	0.58	0.58	1.12
MMP-11								--	1.57	1.54	1.74
MMP-12									--	0.55	1.09
MMP-13										--	0.97
MMP-16											--
mean RMSD	0.99	1.91	1.01	1.24	1.05	1.12	0.99	1.66	0.99	0.91	1.27

(A) The alignment and the 3D superimposition were accomplished by using the *Combinatorial Extention* (CE) algorithm [171], between MMP-1 (template) (PDB code: 1hfc) and the most common MMPs. The Distance Matrix for the whole dataset was calculated, using pairwise alignment sequence. This table lists the average of the distances between two pairs of sequences.

(B) CE Alignments

MMP	Length	RMSD	Gaps	Identity
MMP-2 (1hov)	153	1.86	0	57.5%
MMP-11 (1hv5)	154	1.49	1	55.5%
MMP-3 (1hy7)	151	0.68	3	61.4%
MMP-7 (1mmq)	156	0.96	3	55.4%
MMP-10 (1q3a)	155	0.75	3	61.9%
MMP-16 (1rm8)	156	1.11	12	51.9%
MMP-12 (1y93)	155	0.69	2	59.4%
MMP-8 (1zvx)	155	0.70	2	67.1%
MMP-9 (2ovx)	154	0.92	1	53.9%
MMP-13 (830c)	155	0.63	2	58.2%

(B) Summary of the alignment parameters. Length means the number of aligned aminoacids. RMSD is the root mean square deviation calculated on the C_α atoms. Gaps are the number of the gaps found in the aligned sequence. Identity is expressed as % of similarity between MMP-1 and the remain MMPs.

technique to the loops conformation in the formation of complexes can be a powerful approach to study MMP functional specificity and flexibility. Homology modeling has highlighted the role of specific structural determinants in MMP recognition [168].

An interesting example of this approach is represented by the model of CdMMP-3 complexed with biphenyl inhibitors containing carboxylic acid Zn²⁺ ion-chelating groups, it was built through homology model [110] taking the 3D structure of the related MMP-3/diphenylpiperidine complex (1caq.pdb in Table 1A) as the template. The inhibitor binding mode derived from the molecular model built by structural homology has been confirmed later by X-ray analysis [127].

A homology model of the MMP-26 catalytic domain, whose structure has not been solved, was constructed using the crystal structure of the MMP-12 complexed with the Batimastat inhibitor (**8** in Table 2) as the template (1jk3.pdb, see Table 1A) [175]. Consistent with other MMP family members, the unprimed (left) side of the MMP-26 active site is relatively flat, while the primed (right) side extends deeper into the surface, with a well defined S'₁ pocket formed by residues Leu²⁰⁴, His²⁰⁸ and Tyr²³⁰. Interestingly, the His²³³ of MMP-26 reduces the volume of the S'₁ pocket. Protein sequence analysis suggests that the equivalent residue at position 233 is hydrophilic for MMPs characterized by a S'₁ pocket of intermediate size (i.e. MMP-2, MMP-9 and MMP-8) and hydrophobic in deep-pocket MMPs (i.e., MMP-3, MMP-12 and MMP-14). This observation reinforces the idea that protein sequence analysis and molecular modeling indeed are useful tools to provide new structural insights that may help to distinguish between MMPs with a deep S'₁ pocket from those characterized by a S'₁ pocket of intermediate size [175].

5. STRUCTURE-FUNCTION RELATIONSHIPS OF MMPs

5.1. General Mechanistic Aspects

MMPs catalyze the cleavage of a peptide bond by a mechanism which is similar to that reported for serine and cysteine proteinases although different groups accomplish the electrophilic attack. In MMPs, the catalytic Zn²⁺ ion is coordinated by the three His residues; in the absence of a substrate or an inhibitor, a water molecule (i.e., the catalytic water) is coordinated by the Zn²⁺ ion, being entrapped between the metal and the catalytic Glu residue belonging to the His-Glu-Xxx-Xxx-His-Xxx-Xxx-Gly-Xxx-Xxx-His motif. In all MMPs, the carbonyl group of the scissile peptide bond points towards the catalytic Zn²⁺ ion and therefore can be polarized. The peptide hydrolysis is assisted also by the relatively high pK_a of the carboxyl group of the catalytic Glu residue, which becomes protonated at neutral pH, increasing the hydroxyl character of the catalytic water molecule [176]. This feature facilitates the nucleophilic attack of the water molecule on the carbonyl carbon atom of the scissile peptide bond, which has a carbocationic character due to the polarization induced by the Zn²⁺ ion, giving rise to the tetrahedral intermediate stabilized by both the Zn²⁺ ion and a carbonyl group of a nearby peptide bond. The production of the tetrahedral intermediate leads to the cleavage of the peptide bond

when a second residue (usually His) donates a hydrogen atom to the nitrogen atom of the imido portion of the peptide bond [177]. This sequence of events is confirmed by the dramatic reduction of the MMP activity following the Glu residue mutation [178]. A consequence of this protonation/deprotonation sequence of events is a complex pH-dependence of the enzymatic mechanism, which has been investigated in several MMPs [179,180]; in particular, site-directed mutagenesis has allowed to identify in MMP-3 the crucial role of His²²⁴ as a proton donor [181,182].

A large fraction of functional studies on the enzymatic activity by MMPs has been carried out employing synthetic fluorogenic peptidic substrates [183,184]. These peptides were usually based on the amino acid sequences of natural substrates, such as collagens, aiming to identify the substrate specificity pocket (see ref. [185] for a review). Although a comprehensive overview of all these studies is off the scope for this review, it is important to underline that this approach turned out to be very useful for the identification of the substrate recognition and the cleavage process in the immediate environment of the active site. In this respect, as a very limited example of the relevant informations obtained we can mention that (i) in the case of the two collagenases MMP-1 and MMP-8 the residue in position P'₁ has been shown to play a crucial discriminatory effect, since an aromatic residue in this position renders the synthetic peptide a much better substrate for MMP-8 with respect to MMP-1 [186]; (ii) in the case of the two gelatinases MMP-2 and MMP-9 a substrate selectivity (in favour of MMP-2, see ref. [187]) could be achieved only by the simultaneous presence of a rather hydrophobic residue in the P'₁ position and a positively charged residue (e.g., Arg) in the P₂ position.

Further, investigations on the cleavage of structured synthetic substrates, derived from short triple-helical collagen-like peptides [188], have clearly shown that the thermal stability of triple-helical synthetic substrates is a crucial aspect of the catalytic and recognition mechanism of MMPs [189].

Although these investigations indeed have been of the utmost importance for i) the definition of the mechanistic steps of the proteolytic action by MMPs, ii) the characterization of protonating groups involved in the peptide bond cleavage [180,184] and iii) the identification of substrate recognition pockets in the close proximity of the active site, this information is not enough to account for the actual enzymatic activity of MMPs toward macromolecular substrates. As an example of this, proteolytic cleavage of triple-helical collagen I-like peptides by collagenases is much more efficient than for stromelysins (e.g., MMP-3, see ref. [185]), but this difference did not explain the inability of MMP-3 to process macromolecular collagen I. Thus, functional observations on natural macromolecular substrates, such as collagens, clearly indicated that additional domains (though not directly involved in the enzymatic cleavage chemistry) are very important for substrate recognition and the enzymatic activity on macromolecules [15,17,27].

5.2. Macromolecular Substrates

In the last years, evidence has been emerging that when MMPs interact with macromolecular substrates the correct active-site positioning is achieved through exosite interac-

tions [15,17,27]. Exosites are sites topologically distinct from the catalytic active site (where the substrate cleavage process takes place), they can be located also in additional domains of the MMP, playing a crucial role in the dynamic unfolding of inaccessible regions of substrates (otherwise uncleavable).

The enzymatic activity of several MMPs on different natural substrates, such as collagen I, II and IV has been investigated by several groups [17,28,30,190-192], unravelling various functional features, which imply an important role of different domains in the macromolecular substrate proteolytic processing. Notably, MMP cleavage of bioactive substrates is temperature-dependent [17,180], as also supported by the experiments on triple-helical synthetic substrates [189]. Therefore, in order to derive useful informations for "in vivo" studies we think that 37° C should be the best experimental temperature to employ.

Collagen I is the major component of the extracellular matrix (ECM) and its monomeric structure is made of a triple helix formed by two α -1 chains and one α -2 chain [193]. Collagenolytic MMPs bind native collagen I *via* their exosites and these interactions expose the individual collagen α chain to the active site cleft of the enzyme for the cleavage process, since the intact triple helix cannot enter the active site. In the case of collagenases (i.e., MMP-1, MMP-8 and MMP-13) and of the MT-MMPs (such as MMP-14) the haemopexin-like C-terminal domain turns out to be very important for collagen I binding [28, 30], such that its removal (leaving only the catalytic domain) brings about an altered collagen I cleavage process [15,17]. Further, the binding affinity can be either closely similar for the two chains (as in MMP-8, see ref. [30]) or somewhat higher for the α -2 chain (as in MMP-1 and MMP-13, see ref. [194] and Coletta *et al.* personal communication). On the other hand, the haemopexin-like domain does not seem to play a relevant role in substrate recognition by gelatinases, since its removal does not alter appreciably the collagen I binding [190], whereas substrate recognition for these MMPs occurs preferentially through the fibronectin-like domain [28]. On the other hand, the haemopexin-like domain of gelatinases (and in particular of MMP-2) appears to be connected instead to the lateral mobility of the enzyme along the collagen fibril surface [195]. Unlike the haemopexin-like domain of collagenases (see above), the fibronectin-like domain of gelatinases shows a much higher affinity for the α -1 chain [28, 30], clearly indicating that the structural bases for the interaction of the two types of MMPs with collagen I are different, likely involving different regions of the substrate molecule. In addition, while the interaction of haemopexin does not bring about gross conformational changes of the triple helix of collagen I [28,196], fibronectin-like domain binding induces a substantial unwinding of the triple helix [28,30]. These features result in a dramatically different enzymatic mechanism between collagenases and gelatinases (in particular MMP-2) for collagen I [30], which leads in one case (i.e., for collagenases) to a specific cleavage site (giving rise to the formation of two fragments, corresponding to about $\frac{1}{4}$ and $\frac{3}{4}$ of the collagen chain length, [197], while in the other case (i.e., for gelatinases) a widespread multiple fragmentation of the collagen molecule takes place [30] (Fig. 9). An additional structural element, which comes into play only for macromolecular

substrates, is represented by the linker region, which however does not affect the collagen recognition process, but the enzymatic cleavage process [37]. This feature indeed suggests that after the substrate recognition by collagenases through the haemopexin-like domain the enzymatic activity requires a flexible linker region to correctly position the catalytic domain onto the substrate cleavage site (Fig. 9). This requirement seems also confirmed by the fact that the inability of MMP-3 to enzymatically process collagen I can be bypassed by substituting the region at the edge between the catalytic domain and the linker region with MMP-1 amino acid sequence [27].

Also in the case of collagen IV (the major component of the basement membrane, [198] the role of additional domains (beside the catalytic one) seems to be very important, since binding of substrate by gelatinases indeed occurs *via* the interaction of the substrate with the fibronectin-like domain [199].

5.3. A Strategy for Inhibitor Design Based on Synthetic and Macromolecular Substrates

The elements which are usually taken into consideration for the evaluation of the inhibitor quality are: *i*) the inhibition efficiency (as determined by its dissociation constant, which indicates the concentration needed to inhibit the target enzyme) and *ii*) the inhibition specificity (as estimated by the affinity *ratio* with respect to other homologous proteins).

The MMP inhibitor design exploits and follows the detailed structural information of the enzyme-inhibitor interactions available to date (as reviewed above), even though their effectiveness is mostly validated through functional biochemical studies on the inhibitory power toward substrates, which have been shortly reviewed before (see paragraph 5.1). However, the determination of the intrinsic inhibitor dissociation constant for a given enzyme (i.e., K_i , see Table 2), though necessary, is not enough to evaluate the actual inhibitor efficacy toward macromolecular substrates. Thus, in this case the inhibitor efficacy can be only measured on the basis of its capability to impair the enzyme:substrate interaction and/or to delay the efficiency of the catalytic cycle (i.e., the IC_{50}) (see paragraph 5.2). Therefore, since for macromolecular substrates the enzyme:substrate interaction surface can vary for different substrates, the actual inhibitory power of a molecule is dependent on the type of substrate employed.

On the basis of these considerations, the inhibitor(s) design requires a multistep optimization strategy which can be minimally represented by: *i*) an investigation on synthetic substrates to determine and optimize the effective inhibitory constant (i.e., K_i) of a given molecule, accompanied by the structural information of its complex with enzyme, and *ii*) an investigation on natural macromolecular substrates to determine the effective IC_{50} (or 50% residual activity), which represents the actual inhibitor efficacy toward natural macromolecular substrates, which are encountered "in vivo".

The importance of this multistep strategy may be better appreciated if we focus on the activity of macromolecular inhibitors (such as TIMPs), which interact in a different fashion with a given MMP, involving a different interaction sur-

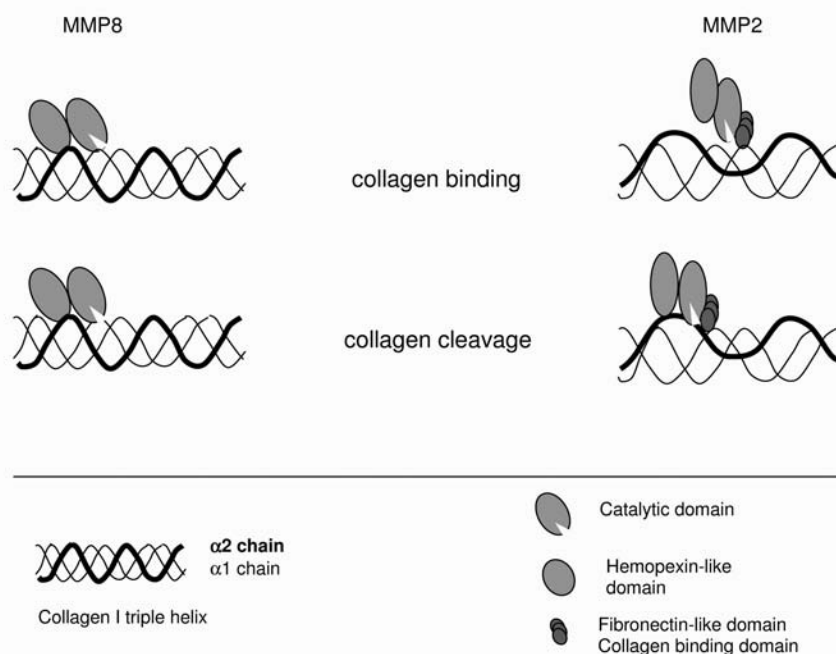


Fig. (9). Collagen I processing by a collagenase and a gelatinase.

Left Panel: sketching of the individual steps for the processing of collagen I by a collagenase. Collagen I interacts with the haemopexin-like domain, without significantly perturbing the triple helix, but positioning the catalytic domain on the the cleavage site of the individual collagen chain.

Right Panel: sketching of the individual steps for the processing of collagen I by a gelatinase. Collagen I interacts with the fibronectin-like domain, inducing the unwinding of the collagen triple helix.

face. Thus, the binding process between MMP-3 and TIMP-1 involves the MMP-3 S₁' pocket [200], while for MMP-2 and/or MMP-9 the interaction with TIMP-1 and TIMP-2 involves the haemopexin-like domains [201].

Therefore, informations on the different mode of binding and enzymatically processing of various natural macromolecular substrates by different MMPs become a crucial point for the accomplishment of a multistep optimization cycle of inhibitor (or drug) design.

As a matter of fact, from studies on macromolecular substrates it emerges that the substrate recognition is mediated by specific exosites of MMPs (mainly through the haemopexin-like domain for collagenases and the fibronectin-like domain for gelatinases), while the catalytic activity, accomplished by the active site, is modulated by the linker region. The macromolecular substrate processing is a multistep process (as depicted in Fig. 9), in which different portions of MMP contribute to different steps.

Therefore, a new "function/structure"-based strategy should be pursued for inhibitor design, mainly focussed on improving the inhibitor efficacy against: *i*) the substrate recognition by additional domain(s) of the MMPs, *ii*) the reciprocal flexibility of tertiary conformations of various domains, and *iii*) the positioning of the residues around the cleavable bond. In this respect, although many excellent inhibitors have been published addressing point *iii*) (see ref. [202] for an extensive review), more attention should be now rather devoted to the design of molecules (likely peptides or

peptidomimetics), which either impair the interaction of additional domains to the macromolecular substrate and/or affect the flexibility of the linker region, interfering with the correct positioning on the substrate of the catalytic domain with respect to the recognition domain (see Fig. 9). In this respect, an interesting work along this line can be considered a recent publication [203], where an efficient inhibition of MMP-2 collagenolysis has been shown by targeting the exosite-substrate interaction.

A different and more complex strategy to be pursued is represented by multifunctional inhibitors able to bind different enzyme domains through their different chemical moieties. In this framework, an initial interesting attempt concerning MMPs has been carried out employing a chimeric protein, consisting of streptavidin fused to a cyclic decapeptide, which has been shown to be a good inhibitor of MMP-2 [204].

In conclusion, a correlated study of structural informations on inhibitor binding to different MMPs and functional behaviour toward natural substrate(s) (such as collagens) triggers a wider and more complete optimization cycle(s) for the efficient and specific inhibitors design.

ACKNOWLEDGEMENTS

The authors are grateful to Hideaki Nagase, Ghislain Opdenakker, Chris Overall, James Quigley, Irit Sagi and Harald Tschesche for fruitful discussions. This study was partly

supported by grants of the Italian Ministry of University and Research (MiUR - COFIN 2003058409 and FIRB RBNE03PX83 to M.C., COFIN 2006068412_003 to S.M.) and of the Italian Space Agency (ASI 2005 OSMA to M.C.).

ABBREVIATIONS

MMP	=	Matrix metalloproteinase
hMMP	=	Human matrix metalloproteinase
CdMMP	=	Catalytic domain of MMP
MT-MMP	=	Membrane-type MMP
TIMP	=	Tissue inhibitor of metalloproteinase
CBD	=	Collagen binding domain
N-TIMP	=	N-terminal region of TIMP
3D	=	Three-dimensional structure
ZBG	=	Zinc Binding Group
CE	=	Combinatorial Extension.

REFERENCES

- Nagase, H.; Woessner, J.F. *J. Biol. Chem.* **1999**, *274*, 21491.
- Vu, T.H.; Werb, Z. *Genes Dev.* **2000**, *14*, 2123.
- Sternlicht, M.D.; Werb, Z. *Annu. Rev. Cell Dev. Biol.* **2001**, *17*, 463.
- Schönbeck, U.; Mach, F.; Libby, P. *J. Immunol.* **1998**, *161*, 3340.
- Van den Steen, P.E.; Proost, P.; Wuyts, A.; Van Damme, J.; Opdenakker, G. *Blood* **2000**, *96*, 2673.
- McQuibban, G.A.; Gong, J.H.; Tam, E.M.; McCulloch, C.A.; Clark-Lewis, I.; Overall, C.M. *Science* **2000**, *289*, 1202.
- Opdenakker, G.; van den Steen, P.E.; Dubois, B.; Nelissen, I.; Van Coillie, E.; Masure, S.; Proost, P.; van Damme, J. *J. Leukoc. Biol.* **2001**, *69*, 851.
- Matrisian, L.M.; Bowden, G.T.; Krieg, P.; Furstenberger, G.; Briand, J.-P.; Leroy, P.; Breathnach, R. *Proc. Natl. Acad. Sci. USA* **1986**, *83*, 9413.
- Hirose, T.; Riefe, R.A.; Smith, G.N.jr.; Stevens, R.M.; Mainardi, C.L.; Hasty, K.A. *J. Rheumatol.* **1992**, *19*, 593.
- Wysocki, A.B.; Staiano-Coico, L.; Grinnell, F. *J. Invest. Dermatol.* **1993**, *101*, 64.
- Bafetti, L.M.; Young, T.N.; Itoh, Y.; Stack, M.S. *J. Biol. Chem.* **1998**, *273*, 143.
- Vu, T.H.; Shipley, J.M.; Bergers, G.; Berger, J.E.; Helms, J.A.; Hanahan, D.; Shapiro, S.D.; Senior, R.M.; Werb, Z. *Cell* **1998**, *93*, 411.
- Opdenakker, G.; Nelissen, I.; van Damme, J. *Lancet Neurol.* **2003**, *2*, 747.
- Fingleton, B. *Curr. Pharm. Des.* **2007**, *13*, 333.
- Murphy, G.; Allan, J.A.; Willenbrock, F.; Cockett, M.I.; O'Connell, J.P.; Docherty, A.J.P. *J. Biol. Chem.* **1992**, *267*, 9612.
- Hirose, T.; Patterson, C.; Pourmotabbed, T.; Mainardi, C.L.; Hasty, K.A. *Proc. Natl. Acad. Sci. USA* **1993**, *90*, 2569.
- Gioia, M.; Fasciglione, G.F.; Marini, S.; D'Alessio, S.; De Sanctis, G.; Diekmann, O.; Pieper, M.; Politi, V.; Tschesche, H.; Coletta, M. *J. Biol. Chem.* **2002**, *277*, 23123.
- Steffensen, B.; Wallon, U. M.; Overall, C. M. *J. Biol. Chem.* **1995**, *270*, 11555.
- Wilson, C.L.; Matrisian, L.N. *Int. J. Biochem. Cell Biol.* **1996**, *28*, 123.
- Marchenko, G.N.; Ratnikov, B.I.; Rozanov, D.V.; Godzik, A.; Deryugina, E.I.; Strongin, A.Y. *Biochem. J.* **2001**, *356*, 705.
- Ohuchi, I.; Imai, K.; Fujii, Y.; Sato, H.; Seiki, M.; Okada, Y. *J. Biol. Chem.* **1997**, *272*, 2446.
- Gill, E.S.; Parks, W.C. *Int. J. Biochem. Cell. B.* **2008**, *40*, 1334.
- Martin, M.D.; Matrisian, L.M. *Cancer Metastasis Rev.* **2007**, *26*, 717.
- Konstantinopoulos, P.A.; Karamouzis, M.V.; Papatsoris, A.G.; Papavassiliou, A.G. *Int. J. Biochem. Cell B* **2008**, *40*, 1156.
- Coussens, L.; Fingleton, B.; Matrisian, L.N. *Science* **2002**, *295*, 2387.
- Overall, C.M.; Kleinfeld, O. *Nat. Rev. Cancer* **2006**, *6*, 227.
- Chung, L.; Shimokawa, K.; Dinakarpanian, D.; Grams, F.; Fields, G.B.; Nagase, H. *J. Biol. Chem.* **2000**, *275*, 29610.
- Tam, E.R.; Moore, T.D.; Butler, G.S.; Overall, C.M. *J. Biol. Chem.* **2004**, *279*, 43336.
- Hu, J.; van den Steen, P.E.; Sang, Q.-X.A.; Opdenakker, G. *Nat. Rev. Drug Discov.* **2007**, *6*, 480.
- Gioia, M.; Monaco, S.; Fasciglione, G.F.; Coletti, A.; Modesti, A.; Marini, S.; Coletta, M. *J. Mol. Biol.* **2007**, *368*, 1101.
- Chow, A.K.; Cena, J.; Schulz, R. *Br. J. Pharmacol.* **2007**, *152*, 189.
- Bhat, T.N.; Bourne, P.; Feng, Z.; Gilliland, G.; Jain, S.; Ravichandran, V.; Schneider, B.; Schneider, K.; Thanki, N.; Weissig, H.; Westbrook, J.; Berman, H.M. *Nucleic Acids Res.* **2001**, *29*, 214.
- Borkakoti, N. *J. Mol. Med.* **2000**, *78*, 261.
- Bode, W.; Fernandez-Catalan, C.; Tschesche, H.; Grams, F.; Nagase, H.; Maskos, K. *Cell Mol. Life Sci.* **1999**, *55*, 639.
- Maskos, K. *Biochimie* **2005**, *87*, 249.
- Overall, C.M.; Butler, G.S. *Structure* **2007**, *15*, 1159.
- Tsakada, H.; Pourmotabbed, T. *J. Biol. Chem.* **2002**, *277*, 27378.
- Springman, E.B.; Angelton, E.L.; Birkedal-Hansen, H.; Van Wart, H.E. *Proc. Natl. Acad. Sci. USA* **1990**, *87*, 364.
- Skiles, J.W.; Gonnella, N.C.; Jeng, A.Y. *Curr. Med. Chem.* **2001**, *8*, 425.
- Velasco, G.; Pendas, A.M.; Fueyo, A.; Knauper, V.; Murphy, G.; Lopez-Otin, C. *J. Biol. Chem.* **1999**, *274*, 4570.
- Pei, D. *J. Biol. Chem.* **1999**, *274*, 8925.
- Pirard, B. *Drug Discov. Today* **2007**, *12*, 640.
- Whittaker, M.; Floyd, C.D.; Brown, P.; Gearing, A.J.H. *Chem. Rev.* **1999**, *99*, 2735.
- Skiles, J.W.; Gonnella, N.C.; Jeng, A.Y. *Curr. Med. Chem.* **2004**, *11*, 2911.
- Agrawal, A.; Romero-Perez, D.; Jacobsen, J.A.; Villarreal, F.J.; Cohen, S. M. *Chem. Med. Chem.* **2008**, *3*, 812.
- Netzel-Arnett, S.; Fields, G.; Birkedal-Hansen, H.; Van Wart, H.E. *J. Biol. Chem.* **1991**, *266*, 6747.
- Iyer, S.; Visse, R.; Nagase, H.; Acharya, K.R. *J. Mol. Biol.* **2006**, *362*, 78.
- Jozic, D.; Bourenkov, G.; Lim, N.G.; Visse, R.; Nagase, H.; Bode, W.; Maskos, K. *J. Biol. Chem.* **2005**, *280*, 9578.
- Lovejoy, B.; Hassell, A.M.; Luther, M.A.; Weigl, D.; Jordon, S.R. *Biochemistry* **1994**, *33*, 8207.
- Lovejoy, B.; Cleasby, A.; Hassel, A.M.; Longley, K.; Luthe, M.A.; Weigl, D.; McGeehan, G.; McElroi, A.B.; Drewry, D.; Lambert, M.H.; Jordan, S.R. *Science* **1994**, *263*, 375.
- Lowry, C.L.; McGeehan, G.; H. Le Vine V. *Proteins* **1992**, *12*, 42.
- Lovejoy, B.; Welch, A.R.; Carr, S.; Luong, C.; Broka, C.; Hendricks, R.T.; Campbell, J. A.; Walker, K.A.M.; Martin, R.; Van Wart, H.; Browner, M.F. *Nat. Struct. Biol.* **1999**, *6*, 217.
- Borkakoti, N.; Winkler, F.K.; Williams, D.H.; D'Arcy, A.; Broadhurst, M.J.; Brown, P.A.; Johnson, W.H.; Murray, E. J. *Nat. Struct. Biol.* **1994**, *1*, 106.
- Spurlino, J.C.; Smallwood, A.M.; Carlton, D.D.; Banks, T.M.; Vavra, K. J.; Johnson, J.S.; Cook, E.R.; Falvo, J.; Wahl, R.C.; Pulvino, T.A.; Wendoloski, J.J.; Smith, D.L. *Proteins* **1994**, *19*, 98.
- Moy, F.J.; Chanda, P.K.; Cosmi, S.; Pisano, M.R.; Urbano, C.; Wilhelm, J.; Powers, R. *Biochemistry* **1998**, *37*, 1495.
- Moy, F.J.; Pisano, M.R.; Chanda, P.K.; Urbano, C.; Killar, L.M.; Sung, M.; Powers, R. *J. Biomol. NMR* **1997**, *10*, 9.
- Moy, F.J.; Chanda, K.P.; Chen, J.M.; Cosmi, S.; Edri, W.; Skotnicki, J.S.; Wilhelm, J.; Powers, R. *Biochemistry* **1999**, *38*, 7085.
- Li, J.; Brick, P.; O'Hare, M.C.; Skarzynski, T.; Lloyd, L. F.; Curry, V.A.; Clark, I.M.; Bigg, H.F.; Hazleman, B.L.; Cawston, T.E. *Structure* **1995**, *3*, 541.
- Terp, G.E.; Cruciani, G.; Christensen, I.T.; Jørgensen, F.S. *J. Med. Chem.* **2002**, *45*, 2675.
- Moore, W. M.; Spilburg, C. A. *Biochem. Biophys. Res. Commun.* **1986**, *136*, 390.
- Moore, W. M.; Spilburg, C. A. *Biochemistry* **1986**, *25*, 5189.

- [62] Pochetti, G.; Gavuzzo, E.; Campestre, C.; Agamennone, M.; Tortorella, P.; Consalvi, V.; Gallina, C.; Hiller, O.; Tschesche, H.; Tucker, P. A.; Mazza, F. *J. Med. Chem.* **2006**, *49*, 923.
- [63] Matter, H.; Schwab, W.; Barbier, D.; Billen, G.; Haase, B.; Neises, B.; Schudok, M.; Thorwart, W.; Schreuder, H.; Brachvogel, V.; Lonze, P.; Weithmann, K.U. *J. Med. Chem.* **1999**, *42*, 1908.
- [64] Brandstetter, H.; Grams, F.; Glitz, D.; Lang, A.; Huber, R.; Bode, W.; Krell, H.W.; Engh, R. A. *J. Biol. Chem.* **2001**, *276*, 17405.
- [65] Grams, F.; Crimmin, M.; Hinnes, L.; Huxley, P.; Pieper, M.; Tschesche, H.; Bode, W. *Biochemistry* **1995**, *34*, 14012.
- [66] Bode, W.; Reinemer, P.; Huber, R.; Kleine, T.; Schnierer, S.; Tschesche, H. *EMBO J.* **1994**, *13*, 1263.
- [67] Brandstetter, H.; Engh, R.A.; Von Roedern, E.G.; Moroder, L.; Huber, R.; Bode, W.; Grams, F. *Protein Sci.* **1998**, *7*, 1303.
- [68] Campestre, C.; Agamennone, M.; Tortorella, P.; Prezioso, S.; Biasone, A.; Gavuzzo, E.; Pochetti, G.; Mazza, F.; Hiller, O.; Tschesche, H.; Consalvi, V.; Gallina, C. *Bioorg. Med. Chem. Lett.* **2006**, *16*, 20.
- [69] Gavuzzo, E.; Pochetti, G.; Mazza, F.; Gallina, C.; Gorini, B.; D'Alessio, S.; Pieper, M.; Tschesche, H.; Tucker, P. A. *J. Med. Chem.* **2000**, *43*, 3377.
- [70] Betz, M.; Huxley, P.; Davies, S.J.; Mushtaq, Y.; Pieper, M.; Tschesche, H.; Bode, W.; Gomis-Ruth, F.X. *Eur. J. Biochem.* **1997**, *247*, 356.
- [71] Schroder, J.; Henke, A.; Wenzel, H.; Brandstetter, H.; Stammer, H. G.; Stammer, A.; Pfeiffer, W. D.; Tschesche, H. *J. Med. Chem.* **2001**, *44*, 3231.
- [72] Bertini, I.; Calderone, V.; Fragai, M.; Luchinat, C.; Maletta, M.; Yeo, K.J. *Angew. Chem. Int. Ed. Engl.* **2006**, *45*, 7952.
- [73] Reinemer, P.; Grams, F.; Huber, R.; Kleine, T.; Schnierer, S.; Pieper, M.; Tschesche, H.; Bode, W. *FEBS Lett.* **1994**, *338*, 227.
- [74] Grams, F.; Reinemer, P.; Powers, J.C.; Kleine, T.; Pieper, M.; Tschesche, H.; Huber, R.; Bode, W. *Eur. J. Biochem.* **1995**, *228*, 830.
- [75] Stams, T.; Spurlino, J. C.; Smith, D.L.; Wahl, R.C.; Ho, T. F.; Qoronfleh, M.W.; Banks, T.M.; Rubin, B. *Nat. Struct. Biol.* **1994**, *1*, 119.
- [76] Engel, C.K.; Pirard, B.; Schimanski, S.; Kirsch, R.; Habermann, J.; Klingler, O.; Schlotte, V.; Weithmann, K.U.; Wendt, K.U. *Chem. Biol.* **2005**, *12*, 181.
- [77] Johnson, A.R.; Pavlovsky, A.G.; Ortwine, D.F.; Prior, F.; Man, C.F.; Bornemeier, D.A.; Banotai, C. A.; Mueller, W.T.; McConnell, P.; Yan, C.; Baragi, V.; Lesch, C.; Roark, W.H.; Wilson, M.; Datta, K.; Guzman, R.; Han, H.K.; Dyer, R.D. *J. Biol. Chem.* **2007**, *282*, 27781.
- [78] Kohno, T.; Hochigai, H.; Yamashita, E.; Tsukihara, T.; Kanaoka, M. *Biochem. Biophys. Res. Commun.* **2006**, *344*, 315.
- [79] Zhang, X.; Gonnella, N.C.; Koehn, J.; Pathak, N.; Ganu, V.; Melton, R.; Parker, D.; Hu, S. I.; Nam, K. Y. *J. Mol. Biol.* **2000**, *301*, 513.
- [80] Moy, F.J.; Chanda, P.K.; Chen, J.M.; Cosmi, S.; Edris, W.; Levin, J.I.; Powers, R. *J. Mol. Biol.* **2000**, *302*, 671.
- [81] Wu, J.; Rush, III. T.S.; Hotchandani, R.; Du, X.; Geck, M.; Collins, E.; Xu, Z.B.; Skotnicki, J. Levin; J.I.; Lovering, F.E. *Bioorg. Med. Chem. Lett.* **2005**, *15*, 4105.
- [82] Gomis-Ruth, F.X.; Gohlke, U.; Betz, M.; Knäuper, V.; Murphy, G.; Lopez-Otin, C.; Bode, W. *J. Mol. Biol.* **1996**, *264*, 556.
- [83] Blagg, J. A.; Noe, M.C.; Wolf-Gouveia, L.A.; Reiter, L.A.; Laird, E.R.; Chang, S-P.P.; Danley, D.E.; Downs, J.T.; Elliott, N.C.; Eskra, J.D.; Griffiths, R.J.; Hardink, J.R.; Haugeto, A.I.; Jones, C.S.; Liras, J.L.; Lopresti-Morrow, L.L.; Mitchell, P.G.; Pandit, J.; Robinson, R.P.; Subramanyam, C.; Vaughn-Bowser, M.L.; Yocum, S.A. *Bioorg. Med. Chem. Lett.* **2005**, *15*, 1807.
- [84] Botos, I.; Meyer, E.; Swanson, S.M.; Lemaitre, V.; Eeckhout, Y.; Meyer, E.F. *J. Mol. Biol.* **1999**, *292*, 837.
- [85] Mitchell, P.G.; Magna, H.A.; Reeves, L.M.; Lopresti-Morrow, L.L.; Yocum, S.A.; Rosner, P.J.; Geoghegan, K.F.; Hambor, J.E. *J. Clin. Invest.* **1996**, *97*, 761.
- [86] Billinghurst, R.C.; Dahlberg, L.; Ionescu, M.; Reiner, A.; Bourne, R.; Rorabeck, C.; Mitchell, P.; Hambor, J.; Diekmann, O.; Tschesche, H.; Chen, J.; Van Wart, H.; Poole, A.R. *J. Clin. Invest.* **1997**, *99*, 1534.
- [87] Ala-aho, R.; Kähäri, V.-M. *Biochimie* **2005**, *87*, 273.
- [88] Li, J.J.; Nahra, J.; Johnson, A.R.; Bunker, A.; O'Brien, A.; Yue, W.-S.; Ortwine, D.F.; Man, C.-F.; Baragi, V.; Kilgore, K.; Dyer, R.D.; Han, H.-K. *J. Med. Chem.* **2008**, *51*, 835.
- [89] Gooljarsingh, L.T.; Lakdawala, A.; Coppo, F.; Luo, L.; Fields, G.B.; Tummino, P.J. *Protein Sci.* **2008**, *17*, 66.
- [90] Strongin, A.Y.; Collier, I.; Bannikov, G.; Marmer, B.L.; Grant, G.A.; Goldberg, G.I. *J. Mol. Biol.* **1995**, *270*, 5331.
- [91] Ramos-DeSimone, N.; Hahn-Dantona, E.; Siple, J.; Nagase, H.; French, D.L.; Quigley, J.P. *J. Mol. Biol.* **1999**, *274*, 13066.
- [92] Morgunova, E.; Tuttila, A.; Bergmann, U.; Isupov, M.; Lindqvist, Y.; Schneider, G.; Tryggvason, K. *Science* **1999**, *284*, 1667.
- [93] Rowsell, S.; Hawtin, P.; Minshull, C.A.; Jepson, H.; Brockbank, S.M.; Barratt, D.G.; Slater, A.M.; McPheat, W. L.; Waterson, D.; Henney, A.M.; Pauptit, R.A. *J. Mol. Biol.* **2002**, *319*, 173.
- [94] Chen, E.L.; Li, W.; Godzik, A.; Howard, E.W.; Smith, J.W. *J. Biol. Chem.* **2003**, *278*, 17158.
- [95] Pirard, B.; Matter, H. *J. Med. Chem.* **2006**, *49*, 51.
- [96] Libson, A.M.; Gittis, A.G.; Collier, I.E.; Marmer, B.L.; Goldberg, G.I.; Lattman, E.E. *Nat. Struct. Biol.* **1995**, *2*, 938.
- [97] Gohlke, U.; Gomis-Ruth, F.X.; Crabbe, T.; Murphy, G.; Docherty, A.J.; Bode, W. *FEBS Lett.* **1996**, *378*, 126.
- [98] Feng, Y.; Likos, J.J.; Zhu, L.; Woodward, H.; Munie, G.; McDonald, J.J.; Stevens, A.M.; Howard, C.P.; De Crescenzo, G.A.; Welsch, D.; Shieh, H.-S.; Stallings, W.C. *Biochim. Biophys. Acta* **2002**, *1598*, 10.
- [99] Dhanaraj, V.; Williams, M.G.; Ye, Q.-Z.; Molina, F.; Johnson, L.L.; Ortwine, D.F.; Pavlovsky, A.; Rubin, J.R.; Skeeane, R.W.; White, A.D.; Humblet, C.; Hupe, D.J.; Blundell, T.L. *Croat. Chem. Acta* **1999**, *72*, 575.
- [100] Gehrman, M.; Briknarova, K.; Banyai, L.; Patthy, L.; Llinas, M. *Biol. Chem.* **2002**, *383*, 137.
- [101] Shich, H.S.; Stegeman, R.A.; Peacock, L.R.; Stevens, A.M.; Howard, G.A.; DeCrescenzo, J.J.; McDonald, A.W.C.; Stallings, A. *Am. Crystallogr. Assoc. Annu. Meet. Abstr.* **1998**, *25*, 129.
- [102] Elkins, P.A.; Ho, Y.S.; Smith, W.W.; Janson, C.A.; D'Alessio, K.J.; McQueney, M.S.; Cummings, M.D.; Romanic, A.M. *Acta Crystallogr. D.* **2002**, *58*, 1182.
- [103] Cha, H.; Kopetzki, E.; Huber, R.; Lanzendorfer, M.; Brandstetter, H. *J. Mol. Biol.* **2002**, *320*, 1065.
- [104] Tochowicz, A.; Maskos, K.; Huber, R.; Oltenfreiter, R.; Dive, V.; Yiotakis, A.; Zanda, M.; Bode, W.; Goettig, P. *J. Mol. Biol.* **2007**, *371*, 989.
- [105] Becker, J.W.; Marcy, A.I.; Rokosz, L.L.; Axel, M.G.; Burbaum, J.J.; Fitzgerald, P.M.; Cameron, P. M.; Esser, C.K.; Hagmann, W.K.; Hermes, J.D. *Protein Sci.* **1995**, *4*, 1966.
- [106] Natchus, M.G.; Bookland, R.G.; Lauferweiler, M.J.; Pikul, S.; Almstead, N.G.; De, B.; Janusz, M.J.; Hsieh, L.C.; Gu, F.; Pokross, M.E.; Patel, V.S.; Garver, S.M.; Peng, S.X.; Branch, T.M.; King, S.L.; Baker, T.R.; Foltz, D.J.; Mieling, G.E. *J. Med. Chem.* **2001**, *44*, 1060.
- [107] Finzel, B.C.; Baldwin, E.T.; Bryant, Jr. G.L.; Hess, G.F.; Wilks, J.W.; Trepod, C.M.; Mott, J.E.; Marshall, V.P.; Petzold, G.L.; Poorman, R.A.; O'Sullivan, T.J.; Schostarez, H.J.; Mitchell, M.A. *Protein Sci.* **1998**, *7*, 2118.
- [108] Stockman, B.J.; Waldon, D.J.; Gates, J.A.; Scahill, T.A.; Kloosterman, D.A.; Mizsak, S.A.; Jacobsen, E.J.; Belonga, K.L.; Mitchell, M.A.; Mao, B.; Petke, J.D.; Goodman, L.; Powers, E.A.; Ledbetter, S.R.; Kaytes, P.S.; Vogali, G.; Marshall, V.P.; Petzold, G.L.; Poorman, R.A. *Protein Sci.* **1998**, *7*, 2281.
- [109] Steele, D.L.; El-Kabbani, O.; Duntun, P.; Windsor, L.J.; Kammlott, R.U.; Crowther, R.L.; Michoud, C.; Engler, J.A.; Birktoft, J.J. *Protein Eng.* **2000**, *13*, 397.
- [110] Pavlovsky, A.G.; Williams, M.G.; Ye, Q.Z.; Ortwine, D.F.; Purchase, D.C.F.; White, A.D.; Dhanaraj, V.; Roth, B.D.; Johnson, L.L.; Hupe, D.; Humblet, C.; Blundell, T.L. *Protein Sci.* **1999**, *8*, 1455.
- [111] Cheng, M.; De, B.; Almstead, N.G.; Pikul, S.; Dowty, M.E.; Dietsch, C.R.; Dunaway, C.M.; Gu, F.; Hsieh, L.C.; Janusz, M.J.; Taiwo, Y.O.; Natchus, M.G.; Hudlicky, T.; Mandel, M. *J. Med. Chem.* **1999**, *42*, 5426.
- [112] Natchus, M.G.; Bookland, R.G.; De, B.; Almstead, N.G.; Pikul, S. *J. Med. Chem.* **2000**, *43*, 4948.
- [113] Esser, C.K.; Bugianesi, R.L.; Caldwell, C.G.; Chapman, K.T.; Durette, P.L.; Girotra, N.N.; Kopka, I.E.; Lanza, T.J.; Levorse,

- D.A.; MacCoss, M.; Owens, K.A.; Ponpipom, M.M.; Simeone, J.P.; Harrison, R.K.; Niedzwiecki, L.; Becker, J.W.; Marcy, A.I.; Axel, M.G.; Christen, A.J.; McDonnell, J.; Moore, V.L.; Olaszewski, J.M.; Saphos, C.; Visco, D.M.; Hagmann, W.K. *J. Med. Chem.* **1997**, *40*, 1026.
- [114] Cheng, M.; De, B.; Pikul, S.; Almstead, N.G.; Natchus, M.G.; Anastasio, M.V.; McPhail, S.J.; Snider, C.E.; Taiwo, Y.O.; Chen, L.; Dunaway, C.M.; Gu, F.; Dowty, M.E.; Mieling, G.E.; Janusz, M.J.; Wang-Weigand, S. *J. Med. Chem.* **2000**, *43*, 369.
- [115] Almstead, N.G.; Bradley, R.S.; Pikul, S.; De, B.; Natchus, M.G.; Taiwo, Y.O.; Gu, F.; Williams, L. E.; Hynd, B.A.; Janusz, M.J.; Dunaway, C.M.; Mieling, G.E. *J. Med. Chem.* **1999**, *42*, 4547.
- [116] Pikul, S.; Dunham, K.M.; Almstead, N.G.; De, B.; Natchus, M.G.; Taiwo, Y.O.; Williams, L. E.; Hynd, B.A.; Hsieh, L.C.; Janusz, M.J.; Gu, F.; Mieling, G.E. *Bioorg. Med. Chem. Lett.* **2001**, *11*, 1009.
- [117] Chen, L.; Rydel, T.J.; Gu, F.; Dunaway, C.M.; Pikul, S.; Dunham, K.M.; Barnett, B.L. *J. Mol. Biol.* **1999**, *293*, 545.
- [118] Li, Y.C.; Zhang, X.; Melton, R.; Ganu, V.; Gonnella, N.C. *Biochemistry* **1998**, *37*, 14048.
- [119] Van Doren, S.R.; Kurochkin, A.V.; Hu, W.; Ye, Q.Z.; Johnson, L.L.; Hupe, D. J.; Zuiderweg, E.R. *Protein Sci.* **1995**, *4*, 2487.
- [120] Pikul, S.; McDow Dunham, K.L.; Almstead, N.G.; De, B.; Natchus, M.G.; Anastasio, M.V.; McPhail, S.J.; Snider, C.E.; Taiwo, Y.O.; Rydel, T.; Dunaway, C.M.; Gu, F.; Mieling, G.E. *J. Med. Chem.* **1998**, *41*, 3568.
- [121] Natchus, M.G.; Cheng, M.; Wahl, C.T.; Pikul, S.; Almstead, N.G.; Bradley, R.S.; Taiwo, Y.O.; Mieling, G.E.; Dunaway, C.M.; Snider, C.E.; McIver, J.M.; Barnett, B.L.; McPhail, S.J.; Anastasio, M.B.; De, B. *Bioorg. Med. Chem. Lett.* **1998**, *8*, 2077.
- [122] Gooley, P.R.; O'Connell, J.F.; Marcy, A.I.; Cuca, G.C.; Salone, S.P.; Bush, B.L.; Hermes, J.D.; Esser, C.K.; Hagmann, W.K.; Sprinter, J.P. *Nat. Struct. Biol.* **1994**, *1*, 111.
- [123] Duntun, P.; Kammlott, U.; Crowther, R.; Levin, W.; Foley, L.H.; Wang, P.; Palermo, R. *Protein Sci.* **2001**, *10*, 923.
- [124] Alcaraz, L.A.; Banci, L.; Bertini, I.; Cantini, F.; Donaire, A.; Gonnelli, L. *J. Biol. Inorg. Chem.* **2007**, *12*, 1197.
- [125] Bertini, I.; Calderone, V.; Fragai, M.; Luchinat, C.; Mangani, S.; Terni, B. *Crystal J. Mol. Biol.* **2004**, *336*, 707.
- [126] Gall, A.L.; Ruff, M.; Kannan, R.; Coniasse, P.; Yiotakis, A.; Dive, V.; Rio, M.C.; Basset, P.; Moras, D. *J. Mol. Biol.* **2001**, *307*, 577.
- [127] O'Brien, P.M.; Ortwine, D.F.; Pavlovsky, A.G.; Picard, J.A.; Sliskovic, D.R.; Roth, B.D.; Dyer, R.D.; Johnson, L.L.; Man, C.F.; Hallak, H. *J. Med. Chem.* **2000**, *43*, 156.
- [128] Matziari, M.; Dive, V.; Yiotakis, A. *Med. Res. Rev.* **2007**, *27*, 528.
- [129] Browner, M.F.; Smith, W.W.; Castelano, A.L. *Biochemistry* **1995**, *34*, 6602.
- [130] Ohnishi, J.; Ohnishi, E.; Jin, M.; Hirano, W.; Nakane, D.; Matsui, H.; kimura, A.; Sawa, H.; Nakayama, K.; Shibuya, H.; Nagashima, K.; Takahashi, T. *Mol. Endocrinol.* **2001**, *15*, 747.
- [131] Park, H.; Turk, B.E.; Gerkema, F.E.; Cantley, L.C. *J. Biol. Chem.* **2002**, *277*, 35168.
- [132] Marchenko, N.D.; Marchenko, G.N.; Strongin, A.Y. *J. Biol. Chem.* **2002**, *277*, 18967.
- [133] Sato, H.; Takino, T.; Okada, Y.; Cao, J.; Shinagawa, A.; Yamamoto, E.; Selki, M. *Nature* **1994**, *370*, 61.
- [134] Wang, Y.; Johnson, A.R.; Ye, Q-Z.; Dyer, R.D. *J. Biol. Chem.* **1999**, *274*, 33043.
- [135] Wang, X.; Yi, J.; Lei, J.; Pei, D. *FEBS Lett.* **1999**, *462*, 261.
- [136] Lang, R.; Braun, M.; Sounni, N.E.; Noel, A.; Frankenne, F.; Foidart, J.M.; Bode, W.; Maskos, K. *J. Mol. Biol.* **2004**, *336*, 213.
- [137] Llano, E.; Pendas, A.M.; Freije, J.P.; Nakano, A.; Knauper, V.; Murphy, G.; Lopez-Otin, C. *Cancer Res.* **1999**, *59*, 2570.
- [138] Morrison, C.J.; Butler, G.S.; Bigg, H.F.; Roberts, C.R.; Soloway, P.D.; Overall, C.M. *J. Biol. Chem.* **2001**, *276*, 47402.
- [139] Fernandez-Catalan, C.; Bode, W.; Huber, R.; Turk, D.; Calvete, J.J.; Lichte, A.; Tschesche, H.; Maskos, K. *EMBO J.* **1998**, *17*, 5238.
- [140] Nar, H.; Werle, K.; Bauer, M.M.T.; Dollinger, H.; Jung, B. *J. Mol. Biol.* **2001**, *312*, 743.
- [141] Bertini, I.; Calderone, V.; Cosenza, M.; Fragai, M.; Lee, Y.-M.; Luchinat, C.; Mangani, S.; Terni, B.; Turano, P. *Proc. Natl. Acad. Sci. USA* **2005**, *102*, 5334.
- [142] Morales, R.; Perrier, S.; Florent, J.M.; Beltra, J.; Dufour, S.; De Mendez, I.; Manceau, P.; Tertre, A.; Moreau, F.; Compere, D.; Dublanquet, A.C.; O'Gara, M. *J. Mol. Biol.* **2004**, *341*, 1063.
- [143] Lang, R.; Kocourek, A.; Braun, M.; Tschesche, H.; Huber, R.; Bode, W.; Maskos, K. *J. Mol. Biol.* **2001**, *312*, 731.
- [144] Bertini, I.; Calderone, V.; Fragai, M.; Luchinat, C.; Maletta, M.; Yeo, K. *J. Angew. Chem. Int. Ed.* **2006**, *45*, 7952.
- [145] Mannino, C.; Nievo, M.; Machetti, F.; Papakyriakou, A.; Calderone, V.; Fragai, M.; Guarna, A. *Bioorg. Med. Chem.* **2006**, *14*, 7392.
- [146] Bertini, I.; Calderone, V.; Fragai, M.; Luchinat, C.; Mangani, S.; Terni, B. *Angew. Chem. Int. Ed.* **2003**, *42*, 2673.
- [147] Bhaskaran, R.; Palmier, M.O.; Bagegni, N.A.; Liang, X.; Van Doren, S.R. *J. Mol. Biol.* **2007**, *374*, 1333.
- [148] Lohi, J.; Wilson, C.L.; Roby, J.D.; Parks, W.C. *J. Biol. Chem.* **2001**, *276*, 10134.
- [149] Marchenko, G.N.; Strongin, A.Y. *Gene* **2001**, *265*, 87.
- [150] Brew, K.; Dinakarpanian, D.; Nagase, H. *Biochim. Biophys. Acta* **2000**, *1477*, 267.
- [151] Maskos, K.; Bode, W. *Mol. Biotechnol.* **2003**, *25*, 241.
- [152] Stamenkovic, I. *J. Pathol.* **2003**, *200*, 448.
- [153] Mott, J.D.; Werb, Z. *Curr. Opin. Cell. Biol.* **2004**, *16*, 558.
- [154] Gomez, D.E.; Alonso, D.F.; Yoshiji, H.; Thorgeirsson, U.P. *Eur. J. Cell. Biol.* **1997**, *74*, 111.
- [155] Murphy, G.; Willenbrock, F. *Methods Enzymol.* **1995**, *248*, 496.
- [156] Verstappen, J.; Von den Hoff, J.W. *J. Dent. Res.* **2006**, *85*, 1074.
- [157] Stetler-Stevenson, W.G.; Bersch, N.; Golde, D.W. *FEBS Lett.* **1992**, *296*, 231.
- [158] Wu, B.; Arumugam, S.; Gao, G.; Lee, G. I.; Semchenko, V.; Huang, W.; Brew, K.; Van Doren, S.R. *J. Mol. Biol.* **2000**, *295*, 257.
- [159] Gomis-Ruth, F. X.; Maskos, K.; Betz, M.; Bergner, A.; Huber, R.; Suzuki, K.; Yoshida, N.; Nagase, H.; Brew, K.; Bourenkov, G.P.; Bartunik, H.; Bode, W. *Nature* **1997**, *389*, 77.
- [160] Arumugam, S.; Van Doren, S.R. *Biochemistry* **2003**, *42*, 7950.
- [161] Iyer, S.; Wei, S.; Brew, K.; Acharya, K.R. *Crystal J. Biol. Chem.* **2007**, *282*, 364.
- [162] Tuuttila, A.; Morgunova, E.; Bergmann, U.; Lindqvist, Y.; Maskos, K.; Fernandez-Catalan, C.; Bode, W.; Tryggvason, K.; Schneider, G. *J. Mol. Biol.* **1998**, *284*, 1133.
- [163] Muskett, F.W.; Frenkiel, T.A.; Feeney, J.; Freedman, R.B.; Carr, M.D.; Williamson, R.A. *J. Biol. Chem.* **1998**, *273*, 21736.
- [164] Kolkenbrock, H.; Orgel, D.; Hecker-Kia, A.; Noack, W.; Ulbrich, N. *Eur. J. Biochem.* **1991**, *198*, 775.
- [165] Morgunova, E.; Tuuttila, A.; Bergmann, U.; Tryggvason, K. *Proc. Natl. Acad. Sci. USA* **2002**, *99*, 7414.
- [166] Maskos, K.; Lang, R.; Tschesche, H.; Bode, W. *J. Mol. Biol.* **2007**, *366*, 1222.
- [167] Andreini, C.; Banci, L.; Bertini, I.; Luchinat, C.; Rosato, A. *J. Proteome Res.* **2004**, *3*, 21.
- [168] Jacobson, M.; Sali, A. *Annu. Rep. Med. Chem.* **2004**, *39*, 259.
- [169] Massova, I.; Kotra, L.P.; Fridman, R.; Mobashery, S. *FASEB J.* **1998**, *12*, 1075.
- [170] Lukacova, V.; Zhang, Y.; Kroll, D.M.; Raha, S.; Comez, D.; Balaz, S. *J. Med. Chem.* **2005**, *48*, 2361.
- [171] Shindyalov, I.N.; Bourne, P.E. *Protein Eng.* **1998**, *9*, 739.
- [172] Kiyama, R.; Tamura, Y.; Watanabe, F.; Tsuzuki, H.; Ohtani, M.; Yodo, M. *J. Med. Chem.* **1999**, *42*, 1723.
- [173] Terp, G.E.; Christensen, I.T.; Jørgensen, F.S. *J. Biomol. Struct. Dyn.* **2000**, *17*, 933.
- [174] Iwata, Y.; Ohiwa, R.; Tamaki, K.; Shibata, T.; Matsubara, A.; Tanzawa, K.; Miyamoto, S. *Chem.-Biol. Inf. J.* **2001**, *1*, 23.
- [175] Park, H.I.; Jin, Y.; Hurst, D.R.; Monroe, C.A.; Lee, S.; Schwartz, M.A.; Sang, Q-X, A. T. *J. Biol. Chem.* **2003**, *278*, 51646.
- [176] Stocker, W.; Bode, W. *Curr. Opin. Struct. Biol.* **1995**, *5*, 383.
- [177] Harrison, R.K.; Chang, B.; Niedzwiecki, L.; Stein, R.L. *Biochemistry* **1992**, *31*, 10757.
- [178] Cha, J.; Auld, D.S. *Biochemistry* **1997**, *36*, 16019.
- [179] Stack, M.S.; Gray, R.D. *Arch. Biochem. Biophys.* **1990**, *281*, 257.
- [180] Fasciglione, G.F.; Marini, S.; D'Alessio, S.; Politi, V.; Coletta, M. *Biophys. J.* **2000**, *79*, 2138.
- [181] Holman, C.M.; Kan, C.-C.; Gehring, M.R.; VanWart, H.E. *Biochemistry* **1999**, *38*, 677.

- [182] Johnson, L.L.; Pavlovsky, A.G.; Johnson, A.R.; Janowicz, J.A.; Man, C.-F.; Ortwine, D.F.; Purchase II, C.F.; White, A.D. *J. Biol. Chem.* **2000**, *275*, 11026.
- [183] Weingarten, H.; Martin, R.; Feder, J. *Biochemistry* **1985**, *24*, 6730.
- [184] Stack, M.S.; Gray, R.D. *J. Biol. Chem.* **1989**, *264*, 4277.
- [185] Nagase, H.; Fields, G.B. *Biopolymers* **1996**, *40*, 399.
- [186] Fields, G.B.; Van Wart, H.E.; Birkedal-Hansen, H. *J. Biol. Chem.* **1987**, *262*, 6221.
- [187] Chen, E.I.; Kridel, S.J.; Howard, E.W.; Li, W.; Godzik, A.; Smith, J.W. *J. Biol. Chem.* **2002**, *277*, 4485.
- [188] Ottl, J.; Gabriel, D.; Murphy, G.; Knäuper, V.; Tominaga, Y.; Nagase, H. *Chem. Biol.* **2000**, *7*, 119.
- [189] Minond, D.; Lauer-Fields, J.L.; Cudic, M.; Overall, C.M.; Pei, D.; Brew, K.; Visse, R.; Nagase, H.; Fields, G.B. *J. Biol. Chem.* **2006**, *281*, 38302.
- [190] Patterson, M.L.; Atkinson, S.J.; Knäuper, V.; Murphy, G. *FEBS Lett.* **2001**, *503*, 158.
- [191] Tam, E.R.; Wu, Y.I.; Butler, G.S.; Stack, M.S.; Overall, C.M. *J. Biol. Chem.* **2002**, *277*, 39005.
- [192] Xu, X.; Wang, Y.; Lauer-Fields, J.L.; Fields, G.B.; Steffensen, B. *Matrix Biol.* **2004**, *23*, 171.
- [193] Prockop, D.J.; Kivirikko, K.I. *Annu. Rev. Biochem.* **1995**, *64*, 403.
- [194] Chung, L.; Dinakarpanian, D.; Yoshida, N.; Lauer-Fields, J.L.; Fields, G.B.; Visse, R.; Nagase, H. *EMBO J.* **2004**, *23*, 3020.
- [195] Collier, I.E.; Saffarian, S.; Marmer, B.L.; Elson, E.L.; Goldberg, G. *Biophys. J.* **2001**, *81*, 2370.
- [196] Marini, S.; Fasciglione, G.F.; De Sanctis, G.; D'Alessio, S.; Politi, V.; Coletta, M. *J. Biol. Chem.* **2000**, *275*, 18657.
- [197] Mallya, S.K.; Mookhtiar, K.A.; Gao, Y.; Brew, K.; Dioszegi, M.; Birkedal-Hansen, H.; van Wart, H.E. *Biochemistry* **1990**, *29*, 10628.
- [198] Kühn, K. *Matrix Biol.* **1995**, *14*, 439.
- [199] Monaco, S.; Sparano, V.; Gioia, M.; Sbardella, D.; Di Pierro, D.; Marini, S.; Coletta, M. *Protein Sci.* **2006**, *15*, 2805.
- [200] Meng, Q.; Malinovsky, V.; Huang, W.; Hu, Y.; Chung, L.; Nagase, H.; Bode, W.; Maskos, K.; Brew, K. *J. Biol. Chem.* **1999**, *274*, 10184.
- [201] Olson, M.W.; Gervasi, D.C.; Mobashery, S.; Fridman, R. *J. Biol. Chem.* **1997**, *272*, 29975.
- [202] Kontogiorgis, C.A.; Papaioannou, P.; Hadjipavlou-Litina, D.J. *Curr. Med. Chem.* **2005**, *12*, 339.
- [203] Xu, X.; Chen, Z.; Wang, Y.; Bonewald, L.; Steffensen, B. *Biochem. J.* **2007**, *406*, 147.
- [204] Farlow, S.J.; Wang, R.J.; Pandori, M.W.; Sano, T. *FEBS Lett.* **2002**, *516*, 197.
- [205] DeLano, W. L. The PyMOL molecular graphics system version 099. DeLano Scientific, San Carlos, CA (<http://www.pymol.org>).
- [206] MOE version 2007.09, Chemical Computing Group. (<http://www.chemcomp.com>).

Received: April 15, 2008

Revised: June 20, 2008

Accepted: June 22, 2008